A VAE FOR TRANSFORMERS WITH NONPARAMETRIC VARIATIONAL INFORMATION BOTTLENECK

Anonymous authors
Paper under double-blind review

ABSTRACT

We propose a Variational AutoEncoder (VAE) for Transformers by developing a Variational Information Bottleneck (VIB) regulariser for Transformer embeddings. We formalise the embedding space of Transformer encoders as mixture distributions, and use Bayesian nonparametrics to develop a Nonparametric VIB (NVIB) for such attention-based representations. The variable number of mixture components supported by nonparametric methods captures the variable number of vectors supported by attention, and exchangeable distributions from nonparametric methods capture the permutation invariance of attention. We then propose our Transformer VAE (NVAE) using NVIB to regularise the information passing from the Transformer encoder to the Transformer decoder through cross-attention. Evaluations of a NVAE, trained on natural language text, demonstrate that NVIB can regularise the number of mixture components in the induced embedding whilst maintaining generation quality and reconstruction capacity.

1 INTRODUCTION

Attention-based deep learning models, such as Transformers (Vaswani et al., 2017; Devlin et al., 2019), have achieved unprecedented empirical success in a wide range of cognitive tasks, in particular in natural language processing. The use of attention allows these models to represent their input with multiple vectors, which is essential for embedding natural language text (Bahdanau et al., 2015). On the other hand, deep variational Bayesian approaches to representation learning, such as variational autoencoders (VAEs) (Kingma & Welling, 2014), have also been shown to have many benefits (Mathieu et al., 2019; Ghosh et al., 2020; Vahdat & Kautz, 2020), especially due to their variational information bottleneck (VIB) (Alemi et al., 2017) for regularising the induced latent representations. However, it has not been clear how to combine these two trends, because the latent space induced by Transformers is a set of vectors whose size grows with the size of the input, whereas standard VIB methods only apply to a vector space of a fixed size (Lin et al., 2020; Fang et al., 2021; Park & Lee, 2021). To define a VIB regulariser for a Transformer's embedding space, we need to allow the size of a latent representation to vary dynamically depending on the complexity of the individual input, and yet regularise the total amount of information conveyed by the whole representation.

In this paper, we propose such a variational information bottleneck for variable sized latent representations, which we use to regularise the embeddings of a Transformer encoder-decoder, giving us a variational autoencoder for Transformers.[1] Like a Transformer's encoder output and decoder input, the proposed VAE's sampled encoder output is (a generalisation of) a set of vectors, and the decoder accesses this embedding with (a generalisation of) cross attention. But unlike Transformers, the proposed VIB layer for this VAE regularises the (effective) number of vectors in the set, as well as the information conveyed by each vector. We show that this regularisation improves generative abilities and compresses latent representations. In addition, previous work shows that VAEs are good for disentanglement (Higgins et al., 2017). All these topics are important and active areas of research in NLP, for efficiency of over-parameterised language models (Child et al., 2019), language generation (Liu & Liu, 2019), and explainability (Mercatali & Freitas, 2021).

To define this VIB, we need to model distributions over these variable-sized encoder embeddings. We argue that these distributions need to be *exchangeable* and *nonparametric*. Firstly, the attention function is insensitive to the order of the vectors in the embedding, so it interprets the output of the encoder as a permutation-invariant set of vectors (Zaheer et al., 2017). Thus, the distributions over these permutation-invariant embeddings should be exchangeable (Jordan, 2010). Secondly, because the attention

[1] We shall release the open source code for this research before publication.

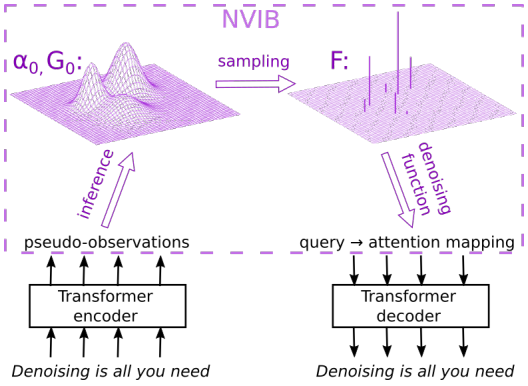

(a) The NVAE model and its NVIB layer.

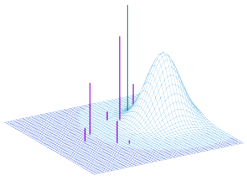

(b) Denoising attention.

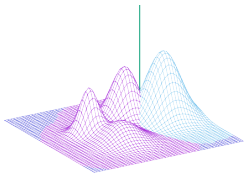

(c) Test-time denoising attention.

Figure 1: (a) Illustration of the NVAE model, with its NVIB layer. (b) Query denoising attention at training time, with the sampled distribution as the query prior, a noisy query observation, and the expected value of the denoised query. (c) Query denoising attention at test time using the mean distribution.

function returns an interpolation between input vectors, it generalises across the varying size of the sets output by the encoder, which like the input length is theoretically unbounded. Thus, to define distributions over these unbounded embeddings, we need to use nonparametric methods (Jordan, 2010).

The properties of permutation-invariance and unboundedness are also shared with mixture probability distributions, which have been extensively studied using Bayesian nonparametric methods with exchangeable distributions (Blei & Jordan, 2006; Jordan, 2010). In previous work, Bayesian nonparametrics is typically applied to learning *models* where the number of parameters grows with the size of the *training data* (Teh, 2010; Jordan, 2010; Kossen et al., 2021). In contrast, we apply it to inferring *latent representations* where the number of parameters grows with the size of the *input*. To the best of our knowledge, ours is the first work to use nonparametric methods in this way for deep variational Bayesian models.

To characterise how attention-based representations are related to mixture distributions, we provide an interpretation of attention where the input set of vectors is interpreted as a mixture of impulse distributions, and the attention function uses this as a prior to denoise the observed query vector (depicted in Figure 1b). Generalising sets of vectors to mixtures of component distributions and generalising the attention function to query denoising allows us to propose a general deep variational Bayesian computational framework for attention-based models using nonparametric methods with exchangeable distributions. More specifically, we propose to use Dirichlet processes (DPs) as the exchangeable distributions (Aldous, 1985; Jordan, 2010) to specify distributions over mixtures of impulse distributions, including distributions over the effective number of components in the mixture.

We define a nonparametric VIB (NVIB) layer using a bounded DP prior and posterior to regularise the effective number of vectors in the latent representation. Applying this NVIB regulariser to a Transformer autoencoder gives us our proposed nonparametric variational autoencoder (NVAE), depicted in Figure 1a. The NVIB layer uses exact inference to infer the posterior from the prior and a set of pseudo-observations output by the encoder, and we propose efficient approximations to sample from this posterior, with their reparameterisation tricks to allow effective backpropagation. The noise introduced by sampling from the DP posterior controls the amount of information which flows from the encoder to the decoder, despite the fact that the amount of information required to reconstruct different text inputs varies enormously.

To evaluate the effectiveness of NVIB, we train a NVAE on natural language text and find that it is able to reconstruct, generate and regularise the effective number of vectors in the latent representation, thereby demonstrating that NVAE is a viable VAE. We also find that the regularised latent space is smooth, using a proposed method for interpolating between DP posteriors to generate interpolations between sentences.

Contributions This paper makes the following contributions: (1) Propose a nonparametric variational Bayesian framework for attention-based representations with *denoising attention* (Section 2). (2) Propose a nonparametric variational information bottleneck (NVIB) regulariser for attention-based representations (Section 3). (3) Propose a nonparametric variational autoencoder (NVAE) which is a variational Bayesian reformulation of a Transformer encoder-decoder (Section 4). (4) Show that the NVAE model is a competitive VAE which can reconstruct, generate, regularise its latent space and intuitively interpolate between sentences (Section 5).

Related work Related work in stochastic attention assume that the keys, queries, values (Martin et al., 2020) or attention weight vectors of the network are treated as latent random variables (Deng et al., 2018; Bah; Fan et al., 2020; Cinquin et al., 2021). Nguyen et al. (2022) provides a formulation and interpretation of attention keys as latent mixture distributions, whereas our formulation characterises the whole attention function and is interpreted as Bayesian query denoising. The use of Bayesian nonparametrics to learn a variable sized latent space using a VAE (Nalisnick & Smyth, 2016; Goyal et al., 2017; Echraibi et al., 2020) still assumes a fixed-sized latent representation at test time, unlike our proposal.

2 Nonparametric Bayesian Framework for Transformer Embeddings

This section proposes a formalisation of attention-based representations as mixture distributions over a vector space, and proposes nonparametric Bayesian methods for modelling information about these mixture distributions. First we show that standard attention functions can be interpreted as implementing Bayesian query denoising, where the set of vectors being accessed specifies a mixture of impulse distributions (Section 2.1). We adopt mixture distributions over vectors as a generalisation of attention-based representations, and adopt this denoising function as a generalisation of attention. Then we use Bayesian nonparametrics to propose prior (Section 2.2) and posterior distributions (Section 2.3) over these mixture distributions. These priors and posteriors form the basis of our nonparametric variational information bottleneck, proposed in Section 3.

2.1 Denoising Attention

The attention function provides access to a set of vectors by mapping a query vector to the resulting attention vector. As the basis of our approach to attention-based representations, we generalise the set of vectors to a probability distribution over vectors, and generalise attention to a function of these probability distributions.

The attention mechanism we assume is scaled dot product attention, standardly used in many attention-based models including Transformers. For simplicity, we consider cross attention, where a single query vector is mapped to a single result vector. This attention function projects the set of vectors $\boldsymbol{Z} \in \mathbb{R}^{n \times p}$ via weight matrices $\boldsymbol{W}^K, \boldsymbol{W}^V \in \mathbb{R}^{p \times d}$ to keys and values, respectively, projects the input $\boldsymbol{u'} \in \mathbb{R}^{1 \times p}$ via the weight matrix $\boldsymbol{W}^Q \in \mathbb{R}^{p \times d}$ to a query, and uses the keys' dimensionality d for scaling. We regroup this scaled dot product attention function into a core dot product attention function $Attn(\boldsymbol{u}, \boldsymbol{Z})$ in which all operations are done in the space of $\boldsymbol{Z}$

$$Attention(\boldsymbol{u'}, \boldsymbol{Z}; \boldsymbol{W}^Q, \boldsymbol{W}^K, \boldsymbol{W}^V) \quad = \quad Attn(\boldsymbol{u'}\boldsymbol{W}^Q(\boldsymbol{W}^K)^T, \boldsymbol{Z})\, \boldsymbol{W}^V \quad = \quad Attn(\boldsymbol{u}, \boldsymbol{Z})\, \boldsymbol{W}^V,$$

where $\boldsymbol{u} = (\boldsymbol{u'}\boldsymbol{W}^Q(\boldsymbol{W}^K)^T) \in \mathbb{R}^{1 \times p}$. The function $Attn(\boldsymbol{u}, \boldsymbol{Z})$ can then be defined in two equivalent ways (as shown in Appendix G), in terms of a sum over the vectors $\boldsymbol{z}_i$ in $\boldsymbol{Z}$, or in terms of an integral over a distribution which is only nonzero at the $\boldsymbol{z}_i$:

$$Attn(\boldsymbol{u}, \boldsymbol{Z}) \quad = \quad \mathrm{softmax}\Big(\tfrac{1}{\sqrt{d}}\boldsymbol{u}\boldsymbol{Z}^T\Big)\boldsymbol{Z} \quad = \quad DAttn(\boldsymbol{u}; F_{\boldsymbol{Z}}) \tag{1}$$

$$F_{\boldsymbol{Z}} \quad = \quad \sum_{i=1}^{n} \frac{\exp(\frac{1}{2\sqrt{d}}||\boldsymbol{z}_i||^2)}{\sum_{i=1}^{n}\exp(\frac{1}{2\sqrt{d}}||\boldsymbol{z}_i||^2)}\, \delta_{\boldsymbol{z}_i} \tag{2}$$

$$DAttn(\boldsymbol{u}; F) \quad = \quad \int_{\boldsymbol{v}} \frac{f(\boldsymbol{v})\, g(\boldsymbol{u}; \boldsymbol{v}, \sqrt{d}\boldsymbol{I})}{\int_{\boldsymbol{v}} f(\boldsymbol{v})\, g(\boldsymbol{u}; \boldsymbol{v}, \sqrt{d}\boldsymbol{I})\, d\boldsymbol{v}}\, \boldsymbol{v}\, d\boldsymbol{v} \tag{3}$$

where $\delta_{\boldsymbol{z}_i}$ is an impulse distribution at $\boldsymbol{z}_i$, $f(\cdot)$ is the probability density function for distribution F, and $g(\boldsymbol{u}; \boldsymbol{v}, \sqrt{d}\boldsymbol{I})$ is the multivariate Gaussian function with diagonal variance of $\sqrt{d}$. As depicted in Figure 1b, $DAttn(u; F_{\boldsymbol{Z}})$ can be interpreted as query denoising. The query $\boldsymbol{u}$ is interpreted as an observation of some true vector $\boldsymbol{v}$ which has been corrupted by Gaussian noise, where $\boldsymbol{v}$ was generated from a prior probability distribution $F_{\boldsymbol{Z}}$ specified by $\boldsymbol{Z}$. The result of $Attn(\boldsymbol{u}, \boldsymbol{Z})$ is the expected value of this true vector $\boldsymbol{v}$ after seeing the noisy observation $\boldsymbol{u}$, which can be interpreted as a form of denoising.

This *denoising attention* function $DAttn(\boldsymbol{u};\, F)$ is actually a generalisation of attention over a set of vectors, in that it is defined for any probability distribution F over a vector space. In the special case where $F = \sum_i \pi_i \delta_{\boldsymbol{z}_i}$ is a finite mixture of impulse distributions, it is the same as $Attn(\boldsymbol{u}, \boldsymbol{Z})$ but with a bias term $\log(\pi_i)$ substituted for $\frac{1}{2\sqrt{d}}||\boldsymbol{z}_i||^2$. In the rest of this paper we will use $DAttn(\boldsymbol{u}; F)$ as our definition of attention, which allows us to treat the latent space of a Transformer encoder-decoder as a mixture distribution.

2.2 A PRIOR OVER MIXTURE DISTRIBUTIONS

Given that our attention-based latent representations are formalised as mixture distributions F, a Bayesian approach requires a prior over these distributions. Attention-based models place no finite bound on the possible number of vectors in their set of vectors $\boldsymbol{Z}$, and thus there is no finite bound on the number of parameters needed to specify the equivalent probability distribution F. Nonetheless, we can still specify distributions $p(F)$ over this infinite space of possible distributions F using methods from Bayesian nonparametrics. These nonparametric Bayesian methods are specifically designed for modelling probability distributions over unboundedly large mixture distributions.

We base our distributions over probability distributions on Dirichlet processes $\mathrm{DP}(G_0,\alpha_0)$. Dirichlet processes (DPs) are a generalisation of Dirichlet distributions to an infinite support, such as the points in a vector space. A Dirichlet distribution $\mathrm{Dir}(\boldsymbol{\alpha})$ is a distribution over probability mass functions $\boldsymbol{\pi}$ of discrete categories i, $1 \leq i \leq \kappa$. One useful definition of Dirichlet processes views a DP $F \sim \mathrm{DP}(G_0,\alpha_0)$, where G_0 is the base distribution over vectors and $\alpha_0 \in \mathbb{R}$ is the concentration parameter, as the limit of a sequence of finite Dirichlet distributions (see Teh (2010)), given in equations 4. Note that the Dirichlet distributions in equations 4 are symmetric, in that all the κ categories i have the same $\alpha_i = \frac{\alpha_0}{\kappa}$ parameter values. However, these categories end up with very different weights π_i, due to the most probable categories getting a large proportion of the probability mass and the tail of categories getting an exponentially decreasing amount of probability mass. In the infinite limit, this tail is infinitely long with infinitesimal probabilities. The number of categories which get nontrivial probabilities is determined by α_0, and becomes independent of κ as κ gets large.

As shown in this definition, each sample F from a DP is an infinite mixture of impulse distributions $\delta_{\boldsymbol{z}_i}$, parameterised by an infinite sequence of weight-vector pairs $\pi_i, \boldsymbol{z}_i$. This contrasts with the finite $\boldsymbol{Z}$ in attention-based representations. The infinite nature of F also causes problems in our variational Bayesian approach. VIB uses a bound on the log-likelihood (the ELBO), which Kingma & Welling (2014) showed has an error of $D_{\mathrm{KL}}(q(F \,|\, x) \parallel p(F \,|\, x))$ (the looseness of the bound), which would be infinite unless both the true posterior $p(F \,|\, x)$ and its approximation $q(F \,|\, x)$ generate a finite mixture F.

$$\begin{aligned} F &= \sum_{i=1}^{\infty} \pi_i \delta_{\boldsymbol{z}_i} \\ \boldsymbol{\pi} &\sim \lim_{\kappa \to \infty} \mathrm{Dir}(\frac{\alpha_0}{\kappa}, \overset{\kappa}{\ldots}, \frac{\alpha_0}{\kappa}) \\ \boldsymbol{z}_i &\sim G_0 \quad \text{for } i = 1, \ldots, \infty \end{aligned} \tag{4}$$

$$\begin{aligned} F &= \sum_{i=1}^{\kappa_0} \pi_i \delta_{\boldsymbol{z}_i} \\ \boldsymbol{\pi} &\sim \mathrm{Dir}(\frac{\alpha_0}{\kappa_0}, \overset{\kappa_0}{\ldots}, \frac{\alpha_0}{\kappa_0}) \\ \boldsymbol{z}_i &\sim G_0 \quad \text{for } i = 1, \ldots, \kappa_0 \end{aligned} \tag{5}$$

The Unbounded Dirichlet Process Prior We do not want a prior which places an apriori bound on the size of $\boldsymbol{Z}$, so we assume it is finite but unbounded, and propose a prior which is an unbounded sequence of finite approximations to a DP. We define a bounded DP $F \sim \mathrm{BDP}(G_0,\alpha_0,\kappa_0)$ as in equations 5. Our approach to the prior is to use an unbounded but finite κ_0, so we define a distribution over approximations as κ_0 increases towards infinity, so that every distribution is over a finite number of vectors, but there is no finite bound on the number of vectors in all distributions. Given ϕ is some distribution over positive integers $\kappa \in \mathbb{Z}^+$, we define this unbounded DP as $\mathrm{UDP}(G_0,\alpha_0,\phi) = \mathrm{BDP}(G_0,\alpha_0,\kappa)$ where $\kappa \sim \phi$.

We use these definitions both to define a general prior over probability distributions, and to define a conditional prior for each input length. In both cases, the base distribution G_0^p is assumed to be a unit Gaussian, inspired by Kingma & Welling (2014), and the concentration parameter α_0^p is assumed to be one.[2]

$$G_0^p = \mathcal{N}(\boldsymbol{\mu}^p, \boldsymbol{I}(\boldsymbol{\sigma}^p)^2); \quad \alpha_0^p = 1; \quad \boldsymbol{\mu}^p = \mathbf{0}; \quad \boldsymbol{\sigma}^p = \mathbf{1}$$

The general prior is $\mathrm{UDP}(G_0^p, \alpha_0^p, \phi^p)$ where the size distribution ϕ^p is determined empirically. The conditional prior $\mathrm{BDP}(G_0^p, \alpha_0^p, \kappa_0)$ sets the level of approximation κ_0 as a fixed function of the input length n, in particular $\kappa_0 = (n+1)\kappa^\Delta$, where $\kappa^\Delta \in \mathbb{Z}^+$ is a hyperparameter that controls the approximation.

A Conditional Bounded DP Prior It will be useful below to generalise this conditioning for the level of approximation to any conditional prior which is a fixed function of only the input length. If we know the input length n, but know nothing about the content of the text, then the distribution of vectors should stay the same as the general prior, $G_0^{p'} = G_0^p$. However, the count of observations we expect to have after an input

[2] We will use "p" and "q" superscripts to designate variables for the prior and posterior, respectively. Similarly, a zero subscript is part of the name of the variable, in contrast to positive integer subscripts which are indices.

of that length would not be α_0^p, but should include a pseudo-count $\alpha^\Delta \in \mathbb{R}_{\geq 0}$ hyperparameter for every token, and thus $\alpha_0^{p'} = \alpha_0^p + n\alpha^\Delta$. This then gives us the conditional prior given n of $\mathrm{BDP}(G_0^p, \alpha_0^{p'}, \kappa_0)$.

2.3 A Posterior over Mixture Distributions

Since a DP is a conjugate prior, we can use exact inference to compute the posterior DP from the prior DP plus a set of pseudo-observations output by the encoder. Each pseudo-observation is a real-valued pseudo-count $\alpha_i^q \in \mathbb{R}_{\geq 0}$ and a parametric distribution which represents uncertainty in the observation. We use an isotropic Gaussian, $G_i^q = \mathcal{N}(\boldsymbol{\mu}_i^q, \boldsymbol{I}(\boldsymbol{\sigma}_i^q)^2)$, as the parametric distribution, specified by a mean $\boldsymbol{\mu}_i^q \in \mathbb{R}^{1\times d}$ and a standard deviation $\boldsymbol{\sigma}_i^q \in \mathbb{R}_{>0}^{1\times d}$. Here we assume that the number of candidate pseudo-observations is the same as the length n of the input, but some of these pseudo-observations may have zero pseudo-counts and thus be effectively removed from the set. The formula for exact inference of the posterior F is given in equations 6, where there is an $n{+}1^{\text{th}}$ component of the base distribution G_0^q which comes from the prior, namely $\alpha_{n+1}^q = \alpha_0^p$ and $G_{n+1}^q = G_0^p$.

$$F \sim \mathrm{DP}(G_0^q, \alpha_0^q) \qquad (6)$$
$$\alpha_0^q = \sum_{i=1}^{n+1} \alpha_i^q \,; \quad G_0^q = \sum_{i=1}^{n+1} \frac{\alpha_i^q}{\alpha_0^q} G_i^q$$

$$F = \sum_{i=1}^{n+1} \rho_i F_i \qquad (7)$$
$$\boldsymbol{\rho} \sim \mathrm{Dir}(\alpha_1^q, \ldots, \alpha_{n+1}^q)$$
$$F_i \sim \mathrm{BDP}(G_i^q, \alpha_i^q, \kappa^\Delta) \quad \text{for } i = 1, \ldots, n{+}1$$

We derive an alternative factorisation of the posterior DP (Appendix H) which helps with the sampling method in Section 3.2. We then bound this factorised DP so that it generates the same number $\kappa_0 = (n{+}1)\kappa^\Delta$ of weighted vectors as the prior $\mathrm{BDP}(G_0^p, \alpha_0^p, \kappa_0)$. The resulting bounded posterior $F \sim \mathrm{BFDP}(\boldsymbol{G}^q, \boldsymbol{\alpha}^q, \kappa^\Delta)$ is given in equations 7, which define our posterior distribution. This posterior simplifies to a mixture $F = \sum_{i=1}^{n+1} \sum_{j=1}^{\kappa^\Delta} \rho_i \pi'_{ij} \delta_{\boldsymbol{z}_{ij}}$ of impulse distributions, with $\boldsymbol{\rho} \sim \mathrm{Dir}(\alpha_1^q, \ldots, \alpha_{n+1}^q)$, $\boldsymbol{\pi}'_i \sim \mathrm{Dir}(\frac{\alpha_i^q}{\kappa^\Delta}, \overset{\kappa^\Delta}{\ldots}, \frac{\alpha_i^q}{\kappa^\Delta})$, and $\boldsymbol{z}_{ij} \sim G_i^q$.

3 The Nonparametric Variational Information Bottleneck

By generalising attention-based representations to mixture distributions and generalising the attention function to denoising attention, we can define a VIB regulariser for attention-based interfaces. We map its input set-of-vectors to a set of pseudo-observations, and we replace its output attention function with denoising attention. Then, given the nonparametric prior and posterior from Section 2, we can define our nonparametric VIB regulariser by specifying: how to compute the KL divergence between prior and posterior; how to effectively sample from the posterior for training; and the mean of these samples to be used at test time. As far as we are aware, this proposal is the first VIB model for attention-based representations like Transformer embeddings.

The VIB layer of a VAE controls the amount of information passing through it by introducing noise according to a posterior output by the encoder, and regularises this information by minimising the KL divergence between this posterior and a prior. One of the known difficulties with VAEs is that they can be difficult to train due to the posterior collapsing to the prior. Similarly to the *free-bits* objective proposed to address this problem for vector-space VAEs (Kingma et al., 2016), instead of regularising towards the prior, which gets no pseudo-counts from the input, we regularise towards the conditional prior $\mathrm{BDP}(G_0^p, \alpha_0^{p'}, \kappa_0)$, which gets $n\alpha^\Delta$ pseudo-counts from the input but knows nothing about the information they convey. We found that this helps with the stability of training and avoiding posterior collapse.

3.1 The Variational Information Bottleneck Loss

The ELBO is commonly used in variational Bayesian methods as an objective which approximately maximises the log-likelihood of the observation x, where here x is the input text.

$$\log(p(x)) \geq \mathbb{E}_{q(F \mid x)} \log(p(x \mid F)) - D_{\mathrm{KL}}(q(F \mid x) \parallel p(F))$$
$$L_R = -\mathbb{E}_{q(F \mid x)} \log(p(x \mid F))$$

The first term of the bound is the reconstruction loss (L_R) computed from samples F from the approximate posterior $q(F \mid x)$, and the second term is the KL divergence between this posterior and the prior $p(F)$.

For the KL divergence term, since both the prior and the posterior are conditioned on the same bound κ_0 on the number of vectors they generate, we can compute a meaningful finite KL divergence between the conditional prior $p(F)$=BDP(G_0^p,$\alpha_0^{p'}$,κ_0) and the posterior $q(F\,|\,x)$=BFDP($\boldsymbol{G}^q$,$\boldsymbol{\alpha}^q$,κ^Δ), given κ^Δ and κ_0=$(n+1)\kappa^\Delta$. The derivation of the KL divergence is given in Appendix I. It has two terms, one (L_D) for the distribution of weights $\boldsymbol{\pi}$ generated by the Dirichlet distributions, and one (L_G) for the distribution of vectors $\boldsymbol{Z}$ generated by the component Gaussians. Using the exact KL divergence for our bounded DPs would regularise each component equally, even for components which have zero α_i^q and thus have no impact on the posterior. We instead approximate a KL divergence where only samples with a nontrivial weight are regularised. Marginalising over the number of nontrivial weights for each component does not appear to be tractable for L_D, but since the relationship is approximately linear (see Appendix I), we simply substitute the expected number $\frac{\alpha_i^q}{\alpha_0^q}\kappa_0$ for the actual number in the equation for KL divergence. This gives us the following loss terms for the KL divergence.

$$
\begin{aligned}
L_D+L_G &\approx D_{\mathrm{KL}}(q(F\,|\,x)\,\|\,p(F)) \qquad (8)\\
L_D &= \log\Gamma(\alpha_0^q)-\log\Gamma(\alpha_0^{p'})+(\alpha_0^q-\alpha_0^{p'})\left(-\psi(\alpha_0^q)+\psi(\frac{\alpha_0^q}{\kappa_0})\right)+\kappa_0\left(\log\Gamma(\frac{\alpha_0^{p'}}{\kappa_0})-\log\Gamma(\frac{\alpha_0^q}{\kappa_0})\right)\\
L_G &= \tfrac{1}{2}\kappa_0\sum_{i=1}^{n+1}\frac{\alpha_i^q}{\alpha_0^q}\sum_{h=1}^{d}\left(\frac{(\mu_{ih}^q-\mu_h^p)^2}{(\sigma_h^p)^2}+\frac{(\sigma_{ih}^q)^2}{(\sigma_h^p)^2}-1-\log\frac{(\sigma_{ih}^q)^2}{(\sigma_h^p)^2}\right)
\end{aligned}
$$

where Γ is the gamma function and ψ is the digamma function. Both L_D and L_G scale approximately linearly with κ_0.

The view of the ELBO as a way to regularise the amount of information which passes through a latent representation allows it to be generalised beyond autoencoders (Alemi et al., 2017). Under this motivation, there is no need for the different parts of the objective to have the same weight. In this paper, we split the ELBO into three parts and introduce two hyperparameters to control the relative weight of these parts, which defines our VIB loss L.

$$L = L_R + \lambda_D L_D + \lambda_G L_G$$

3.2 Sampling a Mixture Distribution from the Posterior

To control the amount of information which passes from the encoder to the decoder, at training time a VAE (Kingma & Welling, 2014) samples from the encoder's posterior distribution and uses this sample to reconstruct the input. The "reparameterisation trick" is used to ensure that backpropagation of the reconstruction error through this sampling step can be done effectively. We propose a novel reparameterisation trick for bounded Dirichlet processes which allows sampling without any categorical choices, and propose specific sampling methods which result in effective backpropagation through the sampling step.

For our NVIB model, we sample the parameters $\langle\boldsymbol{\pi},\boldsymbol{Z}\rangle$ of a mixture distribution F generated by our bounded Dirichlet process posterior BFDP($\boldsymbol{G}^q$,$\boldsymbol{\alpha}^q$,κ^Δ), where F consists of a set of impulse distributions $\delta_{\boldsymbol{z}_k}$ each with a weight π_k. A straightforward approach to sampling from a Dirichlet process would independently sample weights $\boldsymbol{\pi}$ from a (theoretically infinite) Dirichlet distribution and sample vectors $\boldsymbol{Z}$ from the base distribution of the DP, where sampling from the base distribution involves first sampling a component of the base distribution and then sampling a vector from that component's Gaussian.

A Factorised Sampling Method We propose a factorised sampling method where every component of the base distribution has vectors sampled from it an equal (theoretically infinite) number of times, and the only difference between components is the distribution of weights for these different sets of vectors. These weight distributions are specified in the factorised DP in equations 7. Rather than doing a sequence of discrete choices between components, this factorisation of a DP does a continuous choice of a set of weights $\boldsymbol{\rho}$, each one corresponding to the total weight for one component. Each total weight ρ_i is then combined with individual weights $\boldsymbol{\pi}_i'$ and vectors $\boldsymbol{Z}_i$ sampled for each component independently.

Reparameterisation trick The factorised sampling allows for independent sampling of weights and components. Since our components use Gaussian distributions over vectors, we can use the same reparameterisation trick as Kingma & Welling (2014) for sampling vectors $\boldsymbol{Z}_i$ from an individual component i. The bounded nature of our posterior BFDP($\boldsymbol{G}^q$,$\boldsymbol{\alpha}^q$,κ^Δ) means that the total weights $\boldsymbol{\rho}$ and the individual weights $\boldsymbol{\pi}_i'$ are all sampled from Dirichlet distributions. A Dirichlet distribution over a set of category weights can be sampled by sampling from a Gamma distribution for each category and then normalising.

There is no closed-form, explicit reparameterisation trick for the exact Gamma distribution, but there are for approximations. Knowles (2015) proposes two such approximations which we combine, one which is more accurate for small α and one which is more accurate for larger α. We leave the investigation of implicit reparameterisation gradients (Figurnov et al., 2018), an alternative approach to explicit reparameterisation, to future work. More specifics about the sampling methods and their reparameterisation tricks is given in Appendix J. We provide an ablation (Appendix B.3) showing that $\kappa^{\Delta}{=}1$ is an efficient and effective sampling method. In this case, there is no need to sample from the Dirichlet for each individual component, but we still sample the weights $\boldsymbol{\rho}$ across components.

3.3 The Mean Mixture Distribution at Test Time

During test time evaluation, instead of sampling, VAEs typically use the mean of the sampling distribution, which is the base distribution G_0^q for our BFDP posterior. Despite the base distribution being a continuous distribution, whereas at training time all samples are discrete distributions, when accessed via denoising attention the base distribution looks like a typical sample from the posterior. This is visualised in Figure 1 by comparing the vector returned by denoising attention (in green) given the continuous mean distribution (Figure 1c) and a typical sample from this distribution (Figure 1b). Thus, the function defined by applying denoising attention to a sampled distribution can be seen as a noisy version of the function defined by applying denoising attention to the mean distribution. For our Gaussian mixture base distribution G_0^q, there is a closed-form solution to computing denoising attention, given in Appendix F .

4 The Nonparametric Variational Autoencoder

We define a VAE for Transformers by using the nonparametric VIB defined in Section 3 to regularise the attention-based representation between the encoder and decoder of a Transformer autoencoder, as depicted in Figure 1a. In this NVAE model, the Transformer encoder is used to estimate the parameters $\langle \boldsymbol{\alpha}^q, \boldsymbol{\mu}^q, \boldsymbol{\sigma}^q \rangle$ of the posterior given the input text x. The Transformer decoder is used to reconstruct the input text x using denoising attention over a sample F from this posterior.

The NVIB Regulariser Our NVIB layer regularises the amount of information which passes from the encoder to the decoder through this posterior. As with VIB for vector spaces, the KL divergence encourages the encoder to output component Gaussians with smaller $\boldsymbol{\mu}_i^q$ and larger $\boldsymbol{\sigma}_i^q$. With NVIB, the KL divergence also encourages the encoder to output smaller and sparser α_i^q, which regularises the effective number of components in the posterior as well as the noisiness of their weights.

The Transformer Encoder The Transformer encoder $q(F|x)$ with a text x of n number of tokens is used to compute a vector for each token i of the input. From each of these n individual token embeddings, the encoder then linearly projects to three parameters, $\alpha_i^q \in \mathbb{R}$, $\boldsymbol{\mu}_i^q \in \mathbb{R}^{1\times d}$ and $\log(\boldsymbol{\sigma}_i^q) \in \mathbb{R}^{1\times d}$. The variance parameters are exponentiated to be strictly positive, whereas the pseudo-count parameters α_i^q are estimated using a Rectified Linear Unit (ReLU) activation (Nair & Hinton, 2010), which results in masking the vector during cross-attention when it is exactly zero. Thus, the DP posterior has one component $\langle \alpha_i^q, \boldsymbol{\mu}_i^q, \boldsymbol{\sigma}_i^q \rangle$ of its base distribution for each token of the input (plus one for the prior).

The Transformer Decoder The Transformer decoder $q(x|F)$ receives a distribution F over vectors and reconstructs the input text x. During training, F is specified by the sampled vectors $\mathbf{Z} \in \mathbb{R}^{n\times d}$ and the sampled weights $\boldsymbol{\pi} \in \mathbb{R}^{n\times 1}$, and at test time F is specified by the output of the encoder $\boldsymbol{\alpha}^q \in \mathbb{R}^{n\times 1}$, $\boldsymbol{\mu}^q \in \mathbb{R}^{n\times d}$ and $\log(\boldsymbol{\sigma})^q \in \mathbb{R}^{n\times d}$. In both cases, the decoder accesses F using denoising attention in the same way that standard Transformer decoders use cross attention. We include the exact equations used for a deep learning implementation of denoising attention in Appendix K. During training, the text is predicted using teacher forcing, and during test time the text is predicted autoregressively using greedy decoding until the end of sequence token is generated or the sentence generated is 50 tokens larger than the target length.

The Generative Model To use our NVAE model as a generative model, we sample from the prior and use the trained Transformer decoder to generate a sentence. As discussed in Section 2.2, to sample from the same prior as used for training, we need to first sample a sentence length, and then sample from the conditional prior given that (approximate) sentence length. For simplicity, we sample the sentence length from the empirical distribution of sentence lengths in the training data.

5 INTRINSIC EVALUATIONS OF NVIB IN NVAE

To support our theoretical contributions, we demonstrate that our proposed NVIB regulariser performs as predicted. We evaluate it in our proposed NVAE model by training NVAEs on natural language text and evaluating the resulting models. We show that the NVAE is a viable VAE model as it exhibits a competitive reconstruction versus generation trade-off (Section 5.1). We show that the NVIB layer is able to dynamically choose the number of components it needs in its embeddings (Section 5.2). Additionally, NVIB provides an intuitive way to interpolate between sentence embeddings, which provides an evaluation of the smoothness of the latent space (Section 5.3).

Data The Wikitext-2 and Wikitext-103 (Merity et al., 2017) encyclopedia datasets were selected as they are general English language corpora of a small and large scale containing high quality Wikipedia articles.

Baselines We compare to various alternative ways to define a VAE from a Transformer autoencoder. As representative of a standard fixed-length-vector VAE, the Variational Transformer Pooled (VTP) baseline pools its vectors across the sequence length dimension, and then applies a Gaussian VIB layer (Kingma & Welling, 2014). At the other extreme, the Variational Transformer (VT) baseline keeps all its vectors and applies a Gaussian VIB layer to each one. In between these baselines, as a hand-coded solution to constraining the quantity of latent vectors, Variational Transformer Stride (VTS) baselines, with parameter S, masks $1-S$ proportion of the embedding vectors based on their position. For comparability, all our baselines only differ from the NVAE model in the latent representation between the encoder and decoder.

5.1 RECONSTRUCTION VERSUS GENERATION

This section shows that the NVAE Transformer model is a competitive VAE in both reconstruction of input sentences and generation by sampling from the prior. All models undergo hyperparameter tuning on the validation set (Appendix B) across 5 seeds, to select the best models and then report results on the Wikitext-2 test set. For reconstruction, we report the Sacre BLEU metric (Papineni et al., 2002; Post, 2018). For generation, we report forward perplexity (F-PPL) and reverse perplexity (R-PPL) (Zhao et al., 2017; Cífka et al., 2018), which trains an external language model on the gold training text and evaluates it on the generated text (F-PPL) or vice versa (R-PPL). Training details are provided in Appendix A.

Figures 2a and 2b show the reconstruction versus generation trade-off, where lower right is better. The single vector baseline VTP is unable to reconstruct well (low BLEU) or generate diverse sentences (high R-PPL). Even with larger capacity the model performs poorly in generation (Appendix Section B.4). The full vector baseline VT is unable to generate fluent sentences (high F-PPL) whereas the location-based dropout baseline VTS shows that regularisation of the space is beneficial for both reconstruction and generation quality.

The best NVAE models are competitive with the best VTS baselines in being able to both reconstruct and generate, even slightly better at generation with high reconstruction accuracy. In particular, reverse perplexity shows that NVAEs are able to generate a diverse collection of sentences from the prior, and forward perplexity shows that these are fluent sentences (samples in Appendix C). We believe this advantage is the result of learning what vectors to keep instead of a hand-coded location-based dropout.

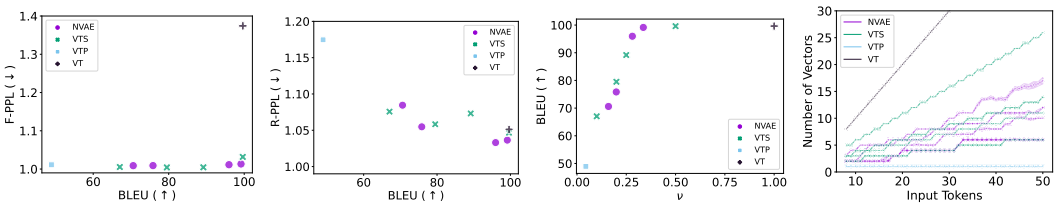

(a) F-PPL vs test BLEU. (b) R-PPL vs test BLEU. (c) Test BLEU vs proportion of retained vectors ν. (d) Latent quantity of vectors vs input tokens.

Figure 2: Reconstruction versus generation trade-off (a), (b) and regularisation analysis (c), (d).

5.2 REGULARISATION

This section shows that the NVIB layer is able to regularise the number of vectors in the latent representation of a NVAE. Without regularisation the NVIB layer becomes a standard transformer without any noise and retaining all latent vectors (Ablation in Appendix Section B.1). The proportion of vectors retained is controllable by the conditional prior hyperparameter α^{Δ}. Figure 2c shows that there exist α^{Δ} where the NVAE is able to remove a significant proportion $(1-\nu)$ of vectors whilst maintaining a high reconstruction performance. Figure 2d plots the number of latent vectors retained during evaluation against the number of input tokens. The NVAE models are able to learn to dynamically regularise the number of vectors based on the information within the text, without hand-coding a function of length as in VTS. The different NVAE lines show the effect of α^{Δ} on vector retention, with larger values allowing more vectors to be used (also see the ablation in Appendix Section B.2).

5.3 INTERPOLATION

The NVIB framework provides an intuitive interpolation between latent sets of vectors that overcomes the challenges with the baselines of latent vector alignment (Ablation in Appendix Section D) and variable set sizes. We simply interpolate the probability assigned to each point in vector space. Given two latent mixture distributions F_1 and F_2, we decode from the combined mixture distribution $(\tau F_1 + (1-\tau)F_2)$, for varying interpolation rates $0 \leq \tau \leq 1$. For the baselines we use $\tau \mathbf{Z}_1 + (1-\tau)\mathbf{Z}_2$ such that the interpolation is over the content of the latent vectors $\mathbf{Z}_i$. We align latent sets of vectors by input position and pad smaller sets with zero vectors, which is the mean of the Gaussian prior. We evaluate the interpolation with selected larger scale models (Ablation in Appendix Section B.4) and use the Wikitext-103 validation set for $\mathbf{S}_1$ and its reverse order for $\mathbf{S}_2$. The results in Table 1 and Figure 3 show that the NVIB regulariser in NVAE provides smoother interpolations, and improvements in fluency of interpolations over the baselines.[3] These finding are qualitatively confirmed through different examples (Appendix Section E).

Model		τ = 0.25	0.5	0.75	**F-PPL** (↓)
VT		0.04	1.00	0.04	$1+1.6e^{-3}$
VTP	$P=max$	0.57	0.99	0.57	$1+3.3e^{-4}$
VTS	$S=0.8$	0.04	1.00	0.04	$1+2.8e^{-3}$
NVAE	$\alpha^{\Delta}=0.4$	0.88	0.89	0.88	$1+1.3e^{-7}$

Table 1: The proportion of interpolations different from $\mathbf{S}_1$ and $\mathbf{S}_2$ by varying the interpolation rate τ. Fluency metric F-PPL of interpolations when $\tau = 0.5$.

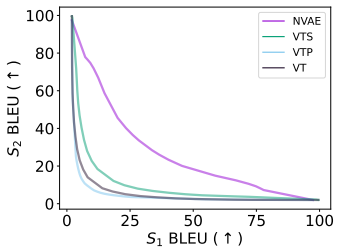

Figure 3: BLEU with $\mathbf{S}_1$ versus $\mathbf{S}_2$ for varying interpolations τ.

6 CONCLUSIONS

In this work, we generalise the latent representations of attention-based models to mixture distributions over a vector space, and propose a nonparametric variational information bottleneck (NVIB) to regularise these latent representations. Using this NVIB model, we propose a nonparametric variational autoencoder (NVAE), which uses a Transformer encoder to embed text in a nonparametric space of distributions over mixture distributions, and uses a Transformer decoder to generate text given a sampled mixture distribution. This nonparametric Bayesian formalisation of attention-based representations captures two key properties of the attention function, namely its invariance to permutations of its input vectors, and that this input can vary widely in size. Our NVIB model adds the ability to regularise attention-based representations so that the size of the representation is appropriate for the complexity of the input being encoded. This is a crucial ability for encoding text, where the size of a text can vary enormously. Empirical evaluations indicate that this model: is a competitive VAE in that it is able to reconstruct input sentences and generate a good distribution over sentences from the prior; regularises the size of the induced latent representations as desired; and is able to intuitively interpolate between latent mixture distributions.

Current work is looking at larger scale experiments. Future work will evaluate the effectiveness of NVIB when applied to multi-head attention and to self-attention layers, and evaluate the usefulness of these pretrained representations in downstream tasks.

[3] F-PPL is calculated across interpolations using a Transformer language model trained on Wikitext-103 at the same scale as the larger models. We remove any collapses to exactly $\mathbf{S}_1$ or $\mathbf{S}_2$ as this will bias the F-PPL metric favourably.

REPRODUCIBILITY STATEMENT

We faithfully describe the details of method in the text and provide detailed derivations for theoretical grounding (Sections G, H,I). We mention all relevant hardware, hyperparameters and datasets to reproduce our experiments (Section A). We provide variance estimations across seeds and ablations to justify design choices (Section B). Finally, we provide exact equations for denoising attention used to make implementation easier (Section K). We shall release the open source code for this research before publication.

REFERENCES

David J. Aldous. Exchangeability and related topics. In P. L. Hennequin (ed.), *École d'Été de Probabilités de Saint-Flour XIII — 1983*, pp. 1–198, Berlin, Heidelberg, 1985. Springer Berlin Heidelberg. ISBN 978-3-540-39316-0.

Alexander A. Alemi, Ian Fischer, Joshua V. Dillon, and Kevin Murphy. Deep variational information bottleneck. In *5th International Conference on Learning Representations, ICLR 2017, Conference Track Proceedings*, Toulon, France, 2017. OpenReview.net. URL https://openreview.net/forum?id=HyxQzBceg.

Dzmitry Bahdanau, Kyunghyun Cho, and Yoshua Bengio. Neural machine translation by jointly learning to align and translate. In Yoshua Bengio and Yann LeCun (eds.), *3rd International Conference on Learning Representations, ICLR 2015, Conference Track Proceedings*, San Diego, CA, USA, May 2015. URL http://arxiv.org/abs/1409.0473.

Hareesh Bahuleyan, Lili Mou, Olga Vechtomova, and Pascal Poupart. Variational attention for sequence-to-sequence models. *CoRR*, abs/1712.08207, 2017. URL http://arxiv.org/abs/1712.08207.

Steven Bird, Ewan Klein, and Edward Loper. *Natural language processing with Python: analyzing text with the natural language toolkit*. " O'Reilly Media, Inc.", 2009.

Christopher M. Bishop. *Neural Networks for Pattern Recognition*. Oxford University Press, Oxford, UK, 1995.

David M Blei and Michael I Jordan. Variational inference for dirichlet process mixtures. *Bayesian analysis*, 1(1):121–143, 2006.

Rewon Child, Scott Gray, Alec Radford, and Ilya Sutskever. Generating long sequences with sparse transformers. *ArXiv*, abs/1904.10509, 2019.

Ondrej Cífka, Aliaksei Severyn, Enrique Alfonseca, and Katja Filippova. Eval all, trust a few, do wrong to none: Comparing sentence generation models. *CoRR*, abs/1804.07972, 2018. URL http://arxiv.org/abs/1804.07972.

Tristan Cinquin, Alexander Immer, Max Horn, and Vincent Fortuin. Pathologies in priors and inference for bayesian transformers. *ArXiv: Computer Science*, abs/2110.04020, 2021.

Yuntian Deng, Yoon Kim, Justin Chiu, Demi Guo, and Alexander Rush. Latent alignment and variational attention. In S. Bengio, H. Wallach, H. Larochelle, K. Grauman, N. Cesa-Bianchi, and R. Garnett (eds.), *Advances in Neural Information Processing Systems*, volume 31. Curran Associates, Inc., 2018. URL https://proceedings.neurips.cc/paper/2018/file/b691334ccf10d4ab144d672f7783c8a3-Paper.pdf.

Jacob Devlin, Ming-Wei Chang, Kenton Lee, and Kristina Toutanova. BERT: Pre-training of deep bidirectional transformers for language understanding. In *Proceedings of the 2019 Conference of the North American Chapter of the Association for Computational Linguistics: Human Language Technologies, Volume 1 (Long and Short Papers)*, pp. 4171–4186, Minneapolis, Minnesota, June 2019. Association for Computational Linguistics. doi: 10.18653/v1/N19-1423. URL https://aclanthology.org/N19-1423.

Amine Echraibi, Joachim Flocon-Cholet, Stéphane Gosselin, and Sandrine Vaton. On the variational posterior of dirichlet process deep latent gaussian mixture models. *ArXiv: Computer Science*, abs/2006.08993, 2020.

Xinjie Fan, Shujian Zhang, Bo Chen, and Mingyuan Zhou. Bayesian attention modules. In H. Larochelle, M. Ranzato, R. Hadsell, M.F. Balcan, and H. Lin (eds.), *Advances in Neural Information Processing Systems*, volume 33, pp. 16362–16376. Curran Associates, Inc., 2020. URL https://proceedings.neurips.cc/paper/2020/file/bcff3f632fd16ff099a49c2f0932b47a-Paper.pdf.

Le Fang, Tao Zeng, Chaochun Liu, Liefeng Bo, Wen Dong, and Changyou Chen. Transformer-based conditional variational autoencoder for controllable story generation. *CoRR*, abs/2101.00828, 2021. URL https://arxiv.org/abs/2101.00828.

Mikhail Figurnov, Shakir Mohamed, and Andriy Mnih. Implicit reparameterization gradients. In S. Bengio, H. Wallach, H. Larochelle, K. Grauman, N. Cesa-Bianchi, and R. Garnett (eds.), *Advances in Neural Information Processing Systems*, volume 31. Curran Associates, Inc., 2018. URL https://proceedings.neurips.cc/paper/2018/file/92c8c96e4c37100777c7190b76d28233-Paper.pdf.

Partha Ghosh, Mehdi S. M. Sajjadi, Antonio Vergari, Michael Black, and Bernhard Scholkopf. From variational to deterministic autoencoders. In *International Conference on Learning Representations*, 2020. URL https://openreview.net/forum?id=S1g7tpEYDS.

Prasoon Goyal, Zhiting Hu, Xiaodan Liang, Chenyu Wang, Eric P. Xing, and Carnegie Mellon. Nonparametric variational auto-encoders for hierarchical representation learning. *2017 IEEE International Conference on Computer Vision (ICCV)*, pp. 5104–5112, 2017.

Irina Higgins, Loïc Matthey, Arka Pal, Christopher P. Burgess, Xavier Glorot, Matthew M. Botvinick, Shakir Mohamed, and Alexander Lerchner. beta-vae: Learning basic visual concepts with a constrained variational framework. In *ICLR*, 2017.

M.I. Jordan. Bayesian nonparametric learning: Expressive priors for intelligent systems. In R. Dechter, H. Geffner, and J. Halpern (eds.), *Heuristics, Probability and Causality: A Tribute to Judea Pearl*, chapter 10. College Publications, 2010.

Diederik P. Kingma and Jimmy Ba. Adam: A method for stochastic optimization. In Yoshua Bengio and Yann LeCun (eds.), *3rd International Conference on Learning Representations, ICLR 2015, San Diego, CA, USA, May 7-9, 2015, Conference Track Proceedings*, 2015. URL http://arxiv.org/abs/1412.6980.

Diederik P. Kingma and Max Welling. Auto-encoding variational bayes. In Yoshua Bengio and Yann LeCun (eds.), *2nd International Conference on Learning Representations, ICLR 2014, Conference Track Proceedings*, Banff, AB, Canada, 2014. URL http://arxiv.org/abs/1312.6114.

Diederik P. Kingma, Tim Salimans, Rafal Józefowicz, Xi Chen, Ilya Sutskever, and Max Welling. Improving variational autoencoders with inverse autoregressive flow. In Daniel D. Lee, Masashi Sugiyama, Ulrike von Luxburg, Isabelle Guyon, and Roman Garnett (eds.), *Advances in Neural Information Processing Systems 29: Annual Conference on Neural Information Processing Systems 2016*, pp. 4736–4744, Barcelona, Spain, 2016. URL https://proceedings.neurips.cc/paper/2016/hash/ddeebdeefdb7e7e7a697e1c3e3d8ef54-Abstract.html.

David A. Knowles. Stochastic gradient variational bayes for gamma approximating distributions. *arXiv: Machine Learning*, 2015. URL https://arxiv.org/abs/1509.01631.

Jannik Kossen, Neil Band, Clare Lyle, Aidan N Gomez, Thomas Rainforth, and Yarin Gal. Self-attention between datapoints: Going beyond individual input-output pairs in deep learning. In M. Ranzato, A. Beygelzimer, Y. Dauphin, P.S. Liang, and J. Wortman Vaughan (eds.), *Advances in Neural Information Processing Systems*, volume 34, pp. 28742–28756. Curran Associates, Inc., 2021. URL https://proceedings.neurips.cc/paper/2021/file/f1507aba9fc82ffa7cc7373c58f8a613-Paper.pdf.

Zhaojiang Lin, Genta Indra Winata, Peng Xu, Zihan Liu, and Pascale Fung. Variational transformers for diverse response generation. *ArXiv*, abs/2003.12738, 2020. URL https://arxiv.org/abs/2003.12738.

Danyang Liu and Gongshen Liu. A transformer-based variational autoencoder for sentence generation. In *2019 International Joint Conference on Neural Networks (IJCNN)*, pp. 1–7. IEEE, 2019.

Alice Martin, Charles Ollion, Florian Strub, Sylvain Le Corff, and Olivier Pietquin. The monte carlo transformer: a stochastic self-attention model for sequence prediction. *ArXiv: Mathematics, Computer Science*, abs/2007.08620, 2020.

Emile Mathieu, Tom Rainforth, N. Siddharth, and Yee Whye Teh. Disentangling disentanglement in variational autoencoders. In *ICML*, 2019.

Giangiacomo Mercatali and André Freitas. Disentangling generative factors in natural language with discrete variational autoencoders. In *EMNLP*, 2021.

Stephen Merity, Caiming Xiong, James Bradbury, and Richard Socher. Pointer sentinel mixture models. In *5th International Conference on Learning Representations, ICLR 2017, Conference Track Proceedings*, Toulon, France, 2017. OpenReview.net. URL https://openreview.net/forum?id=Byj72udxe.

Vinod Nair and Geoffrey E. Hinton. Rectified linear units improve restricted boltzmann machines. In *ICML*, 2010.

Eric Nalisnick and Padhraic Smyth. Stick-breaking variational autoencoders, 2016. URL https://arxiv.org/abs/1605.06197.

Tam Nguyen, Tan Minh Nguyen, Dung Le, Duy Khuong Nguyen, Viet-Anh Tran, Richard Baraniuk, Nhat Ho, and Stanley J. Osher. Improving transformers with probabilistic attention keys. In *ICML*, 2022.

Kishore Papineni, Salim Roukos, Todd Ward, and Wei-Jing Zhu. Bleu: a method for automatic evaluation of machine translation. In *Proceedings of the 40th Annual Meeting of the Association for Computational Linguistics*, pp. 311–318, Philadelphia, Pennsylvania, USA, July 2002. Association for Computational Linguistics. doi: 10.3115/1073083.1073135. URL https://aclanthology.org/P02-1040.

Seongmin Park and Jihwa Lee. Finetuning pretrained transformers into variational autoencoders. In *Proceedings of the Second Workshop on Insights from Negative Results in NLP*, pp. 29–35, Online and Punta Cana, Dominican Republic, November 2021. Association for Computational Linguistics. URL https://aclanthology.org/2021.insights-1.5.

Matt Post. A call for clarity in reporting BLEU scores. In *Proceedings of the Third Conference on Machine Translation: Research Papers*, pp. 186–191, Brussels, Belgium, October 2018. Association for Computational Linguistics. doi: 10.18653/v1/W18-6319. URL https://aclanthology.org/W18-6319.

Yee Whye Teh. Dirichlet processes. In *Encyclopedia of Machine Learning*, volume 1063, pp. 280–287. Springer, 2010.

Arash Vahdat and Jan Kautz. NVAE: A deep hierarchical variational autoencoder. In *Neural Information Processing Systems (NeurIPS)*, 2020.

Ashish Vaswani, Noam Shazeer, Niki Parmar, Jakob Uszkoreit, Llion Jones, Aidan N Gomez, Ł ukasz Kaiser, and Illia Polosukhin. Attention is all you need. In I. Guyon, U. V. Luxburg, S. Bengio, H. Wallach, R. Fergus, S. Vishwanathan, and R. Garnett (eds.), *Advances in Neural Information Processing Systems*, volume 30. Curran Associates, Inc., 2017. URL https://proceedings.neurips.cc/paper/2017/file/3f5ee243547dee91fbd053c1c4a845aa-Paper.pdf.

Manzil Zaheer, Satwik Kottur, Siamak Ravanbakhsh, Barnabás Póczos, Ruslan Salakhutdinov, and Alexander J. Smola. Deep sets. In Isabelle Guyon, Ulrike von Luxburg, Samy Bengio, Hanna M. Wallach, Rob Fergus, S. V. N. Vishwanathan, and Roman Garnett (eds.), *Advances in Neural Information Processing Systems 30: Annual Conference on Neural Information Processing Systems 2017*, pp. 3391–3401, Long Beach, CA, USA, 2017. URL https://proceedings.neurips.cc/paper/2017/hash/f22e4747da1aa27e363d86d40ff442fe-Abstract.html.

Junbo Jake Zhao, Yoon Kim, Kelly Zhang, Alexander M. Rush, and Yann LeCun. Adversarially regularized autoencoders for generating discrete structures. *CoRR*, abs/1706.04223, 2017. URL http://arxiv.org/abs/1706.04223.

A EXPERIMENTAL SETUP

Training details All models are trained, without pretraining using the same encoder and decoder configuration for comparability. We use a two layer Transformer encoder and decoder with a single attention-head. The size for the word embedding vectors and model projections are 256, feed forward dimensions 1024, which leads to models of approximately 19 million trainable parameters. The BERT base-uncased tokeniser is used for tokenisation with a vocabulary of approximately 30K. During training we use: a constant learning rate of $1e^{-4}$, Adam optimiser (Kingma & Ba, 2015), a batch size of 256, gradient norm clipping 0.1 and trained for 50 epochs ($\approx 15K$ steps). The number epochs were selected considering model convergence and minimising computation time. As a form of regularisation we use a dropout rate of 0.1 and the VIB parameters λ_G, λ_D, α^{Δ} and κ^{Δ} are selected through a hyperparameter tuning. Learning rate schedules, KL annealing strategies and free-bits KL loss objectives were considered but unnecessary for convergence. Each model experiment takes approximately 2hrs to on single NVIDIA GeForce RTX 3090.

Generation metrics The two automatic generation metrics forward/reverse perplexity (Zhao et al., 2017; Cífka et al., 2018) both involve training an external language model, for which we use a Transformer language with the same configuration, without VIB regularisation. First we generate 100k sample sentences from the model we wish to evaluate. The forward perplexity (F-PPL) measures the perplexity of the external language model trained on training data and evaluated on the generated text . This measures fluency of the text. The reverse perplexity (R-PPL) measures the perplexity of the external language model trained on generated samples and evaluated on validation or test data. This captures the word frequency and overall proximity of our generated text distribution to the true text distribution.

Data In general the Wikitext-2 dataset, which is a small subset of encyclipedia Wikitext-103 dataset (Merity et al., 2017), is used and we reserve the larger scale data for the larger model experiments (Appendix Section B.4) and interpolations (Section 5.3). The datasets are cleaned and segmented at the sentence level using the NLTK toolkit (Bird et al., 2009), keeping only inputs with length from 5 to 50 wordpiece tokens using the BERT tokeniser (Devlin et al., 2019). Dataset statistics can be found in Table 2.

	Train/Val/Test	**Tokens**
Wikitext-2	$77K/8K/9K$	26 ± 12
Wikitext-103	$3578K/9K/8K$	25 ± 10

Table 2: Dataset statistics.

B HYPERPARAMETER TUNING

The data is trained on the Wikitext-2 training dataset and tuned on the validation with the aim to be able to both reconstruct and generate output. Preliminary experiments suggest that training converges better without this linear dependence on sentence length, so we set the weights on the Gaussian and Dirichlet KL divergences to be linear in $\frac{1}{n}$. In addition we scale the weights on the Gaussian KL divergence by $\frac{1}{d}$, removing the dependence on the dimensionality d of vectors.

$$\lambda_D = \frac{1}{n}\lambda'_D\,; \quad \lambda_G = \frac{1}{d}\frac{1}{n}\lambda'_G$$

All combinations of the following hyperparameters were considered in a grid search for the respective models:

- $\lambda'_G = \{1, 1e^{-1}, 1e^{-2}, 1e^{-3}, 1e^{-4}, 1e^{-5}, 0\}$
- $\lambda'_D = \{10, 1, 1e^{-1}, 1e^{-2}, 1e^{-3}, 1e^{-4}, 1e^{-5}, 0\}$
- $\alpha^{\Delta} = \{1, 0.75, 0.5, 0.4, 0.3, 0.2, 0.1, 0\}$
- $\kappa^{\Delta} = \{1, 2, 5\}$
- $S = \{0.9, 0.8, 0.75, 0.5, 0.25\}$
- $P = \{\text{mean, max, one}\}$

where λ'_G and λ'_D are the weights on the Gaussian and Dirichlet KL divergences for all variational models, respectively. The α^{Δ} and κ^{Δ} are NVAE specific parameters and represent the conditional prior parameter and number of samples per component. The stride parameter S for the VTS model results in $1 - S$ proportion of vectors. Finally, P is the pooling parameter for the single vector model VTP.

Baselines Empirically we found the best KL divergence parameter for VT, VTP and VTS is $\lambda'_G = 1e^{-2}$ and using max pooling for VTP. All stride parameters are considered to adjust the number of vectors. This provides the best trade off of reconstruction accuracy with high BLEU score and generative sampling ability achieved by low F-PPL and R-PPL scores.

NVAE The hyperparameter tuning for NVAE aims to discover models which do not collapse to a single vector or use all vectors, reconstruct and able to sample effectively from the prior by achieving low FPPL and RPPL scores. Empirically we find the parameters $\lambda'_G = 1e^{-3}$, $\lambda'_D = 1$ and $\kappa^{\Delta} = 1$ to produce the best trade off between reconstruction accuracy and generative ability. The α^{Δ} parameter is able to control the proportion of vectors (Appendix Section B.2) retained and $\kappa^{\Delta} = 1$ provides an efficient sampling of the model (Appendix Section B.3).

Validation results Table 3 display the validation reconstruction and generation results across 5 seeds for the best performing parameters. The VT model is able reconstruct well, however a high F-PPL score suggest a poor fluency of generated text and large variation. The VTP models show that a single vector bottleneck is insufficient to reconstruct. Low F-PPL and high R-PPL suggest the model has collapsed to a just sampling a few fluent sentences. We notice that NVAE is able to find comparable models with respects to average proportion of vectors retained ν to the VTS models. Their performance is comparable with respects to reconstruction and generation. However, the NVAE models have notably more variance of metrics across seeds.

Model		ν	Reconstruction			Generation	
			BLEU (↑)	**PPL** (↓)		**F-PPL** (↓)	**R-PPL** (↓)
VT		1.00	99.63±0.00	1.00	±0.00	1.96 ±0.89	1.06 ±0.02
VTS	$S=0.5$	0.50	99.59 ±0.01	1.00	±0.00	1.03 ±0.01	1.06 ±0.01
VTS	$S=0.75$	0.25	88.92 ±0.73	3.74	±0.37	1.00 ±0.00	1.08 ±0.01
VTS	$S=0.8$	0.20	77.99 ±0.63	18.78	±1.41	1.00 ±0.00	1.08 ±0.01
VTS	$S=0.9$	0.10	65.20 ±1.02	66.71	±11.46	1.00 ±0.00	1.09 ±0.01
VTP	$P=max$	0.05*	46.36 ±0.40	1659.24	±70.28	1.01 ±0.00	1.21 ±0.03
VTP	$P=mean$	0.05*	42.94 ±0.49	2425.25	±97.65	1.09 ±0.03	1.35 ±0.02
VTP	$P=one$	0.05*	38.33 ±1.08	2902.39	±456.97	1.00 ±0.00	1.29 ±0.03
NVAE	$\alpha^{\Delta}=1$	0.50 ±0.15	98.90 ±0.67	1.07	±0.07	1.03 ±0.02	1.50 ±0.65
NVAE	$\alpha^{\Delta}=0.75$	0.40 ±0.10	98.19 ±1.87	1.15	±0.21	1.02 ±0.02	1.15 ±0.10
NVAE	$\alpha^{\Delta}=0.5$	0.27 ±0.06	92.78 ±4.61	2.14	±1.06	1.02 ±0.00	1.15 ±0.09
NVAE	$\alpha^{\Delta}=0.4$	0.23 ±0.06	83.93 ±14.58	29.75	±60.42	1.02 ±0.01	1.11 ±0.05
NVAE	$\alpha^{\Delta}=0.3$	0.18 ±0.02	67.01 ±-10.30	119.97	±151.43	1.01 ±0.01	1.12 ±0.09
NVAE	$\alpha^{\Delta}=0.2$	0.13 ±0.03	54.02 ±14.67	1145.56	±1490.82	1.01 ±0.01	1.26 ±0.27
NVAE	$\alpha^{\Delta}=0.1$	0.11 ±0.02	44.46 ±6.59	1635.51	±1122.01	1.01 ±0.00	1.21 ±0.10

Table 3: Results for regularisation and generation on validation Wikitext-2 averaged over 5 seeds. The average proportion of latent vectors retained during evaluation is reported by ν. *The VTP models only use a single vector.

Figures 4c 4a and 4b visually display the reconstruction versus generation trade-off for the validation data across seeds. The best models have both low generation perplexities and high BLEU scores whilst dropping a large proportion of vectors. Figure 4c shows that the NVAE model is able to dynamically reduce the average proportion of vectors and reconstruct comparatively to the VTS model. We notice that their exist some NVAE models that have a good reconstruction-generation trade-off but are less clustered than the VTS models. Note that the R-PPL and F-PPL plot limits are cropped at 1.2 to focus on the higher performing models.

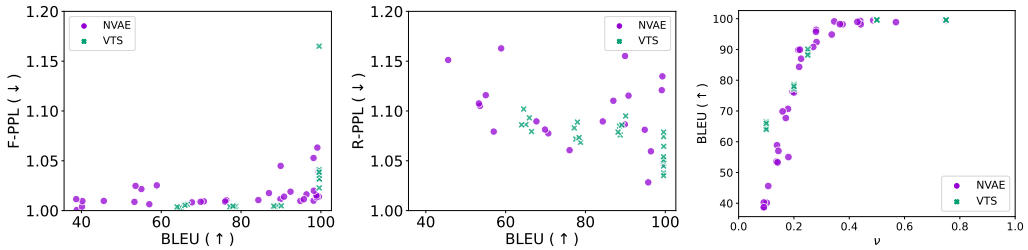

(a) Validation BLEU vs F-PPL. (b) Validation BLEU vs R-PPL. (c) Validation BLEU vs proportion of retained vectors ν.

Figure 4: Reconstruction versus generation trade-off and regularisation for Wikitext-2 validation.

Test results The best seed models from Table 3 are selected for the baselines and NVAE and then evaluated on the test set and shown in Table 4 and a subset of this $\alpha^{\Delta}=\{0.75, 0.4, 0.3, 0.2\}$ is plotted in Figure 2.

Model		ν	Reconstruction		Generation	
			BLEU (↑)	PPL (↓)	F-PPL (↓)	R-PPL (↓)
VT		1.00	99.63	1.00	1.37	1.11
VTS	$S=0.5$	0.50	99.61	1.00	1.03	1.05
VTS	$S=0.75$	0.25	89.18	3.72	1.00	1.07
VTS	$S=0.8$	0.20	79.51	15.51	1.00	1.06
VTS	$S=0.9$	0.10	67.04	51.47	1.01	1.08
VTP	$P=max$	0.05*	48.940	1386.34	1.01	1.17
NVAE	$\alpha^{\Delta}=1$	0.44	99.27	1.04	1.04	1.12
NVAE	$\alpha^{\Delta}=0.75$	0.34	99.15	1.04	1.01	1.04
NVAE	$\alpha^{\Delta}=0.5$	0.28	96.35	1.33	1.02	1.05
NVAE	$\alpha^{\Delta}=0.4$	0.28	95.96	1.41	1.01	1.03
NVAE	$\alpha^{\Delta}=0.3$	0.19	75.83	17.18	1.01	1.05
NVAE	$\alpha^{\Delta}=0.2$	0.16	70.60	23.46	1.01	1.08
NVAE	$\alpha^{\Delta}=0.1$	0.14	54.35	267.59	1.01	1.11

Table 4: Results for regularisation and generation on test Wikitext-2. The average proportion of latent vectors retained during evaluation is reported by $\boldsymbol{\nu}$. *The VTP models only use a single vector.

B.1 No regularisation ablation

In this ablation we consider the behaviour of the NVAE without any regularisation. Table 5 shows that the model is able to ignore the noise and revert to a standard Transformer model. We can see this by the model retaining all its vectors as $\nu=1$ and being able to perfectly reconstruct the input.

Model	ν	Reconstruction	
		BLEU (↑)	PPL (↓)
T	1	99.63 ±0.00	1.00 ±0.00
VT	1	99.63 ±0.00	1.00 ±0.00
NVAE	1	99.63 ±0.00	1.00 ±0.00

Table 5: Reconstuction results on Wikitext-2 validation data without regularisation.

B.2 Conditional prior ablation

In this ablation we consider the affect of the conditional prior α^{Δ}. We select a subset of hyperparameters that managed to achieve good reconstruction and generation performance: $\lambda'_G = \{1e^{-3},\ 1e^{-4}\}$, $\lambda'_D=\{1, 10\}$, $\kappa^{\Delta}=\{1, 2, 5\}$ each across 5 random seed samples.

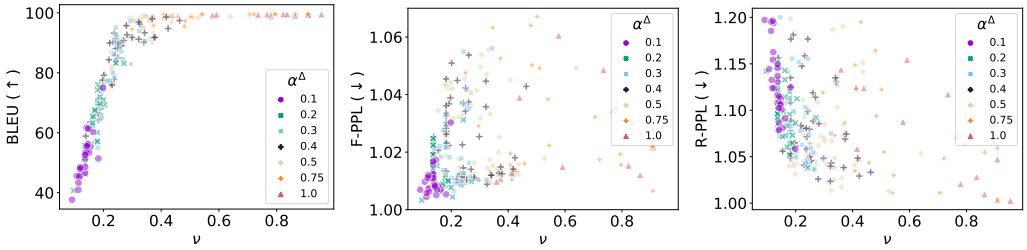

(a) Validation BLEU vs proportion of retained vectors ν.

(b) Validation F-PPL vs proportion of retained vectors ν.

(c) Validation R-PPL vs proportion of retained vectors ν.

Figure 5: Conditional prior α^{Δ} controlling the proportion of retained vectors ν.

The figures shows validation reconstruction BLEU against the average proportion of vectors ν is controlled by the conditional prior α^{Δ} across these parameters. The parameter α^{Δ} roughly corresponds to the proportion of vectors you wish to retain making the models regularisation controllable.

B.3 NUMBER OF SAMPLES ABLATION

In this ablation we consider the affect of the number of samples κ^{Δ} per component. We consider a subset of hyperparameters $\lambda'_G = \{1e^{-3}, 1e^{-4}\}$, $\lambda'_D = \{1, 10\}$, $\alpha^{\Delta} = \{0.1, 0.2, 0.3, 0.4, 0.5, 0.75, 1\}$ each across 5 random seed samples.

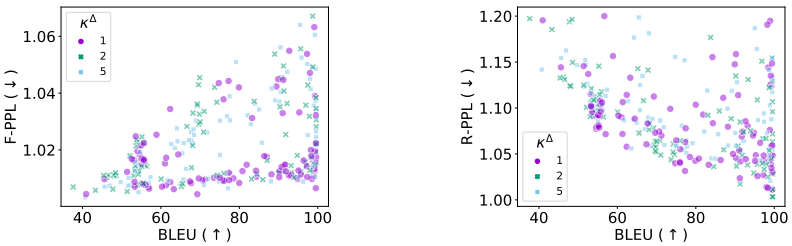

(a) Validation BLEU vs F-PPL.

(b) Validation BLEU vs R-PPL.

Figure 6: Number of samples κ^{Δ} reconstruction and generation trade off.

The figures shows validation generation metrics F-PPL and R-PPL against reconstruction BLEU for a different number of samples κ^{Δ} per component does not have a significant improvement in the generation or reconstruction ability of the models. Hence, we use a single sample $\kappa^{\Delta} = 1$ per component.

B.4 LARGER SCALE ABLATION

We conduct a larger scale experiment to if NVIB is able to generalise to models with more parameters and larger datasets such as Wikitext-103. Due to restricted resources we needed to be selective with the larger scale experimentation. We scale up the models (inspired by the Transformer base size (Vaswani et al., 2017)) by using six layer Transformer encoder and decoder with the word embedding vectors and model projections are 512, feed forward dimensions 2048, which leads to models of approximately 76 million trainable parameters. We use a constant learning rate of $1e^{-5}$ and trained for 11 epochs ($\approx 150K$ steps). Each model experiment takes approximately 24hrs to on a single NVIDIA Tesla v100 which was the largest compute within budget. Otherwise the same training details of Appendix Section A are used.

We initially trained the NVAE model with the best parameters (based on lowest R-PPL score) from Table 4 thereafter we trained the VTS model with the closest proportion of vectors retained for comparability.

			Reconstruction		**Generation**	
Model		ν	**BLEU** (↑)	**PPL** (↓)	**F-PPL** (↓)	**R-PPL** (↓)
VT		1.00	99.56	1.00	1.06	1.08
VTP	$P = max$	0.05*	97.42	1.54	2.41	1.01
VTS	$S = 0.8$	0.20	99.52	1.00	1.04	1.01
NVAE	$\alpha^{\Delta} = 0.4$	0.15	99.51	1.01	1.01	1.01

Table 6: Results for large scale models for regularisation and generation on test Wikitext-103.

In Table B.4 we see that with larger model capacity allows the VTP models to be more competitive in reconstruction however, still struggles in generation. The NVAE model is able to dynamically regularise more vectors and is competitive with the baselines at scale with respects to both reconstruction and generation.

C GENERATED SAMPLE EXAMPLES

	Samples (Wikitext-2)
VT	• each fought..'considered in per resulting corps.
$\lambda'_G = 1e^{-2}$	• video game,s's reprinted le nes 2010 allowing track video game, browns passengers for the third race, [UNK] he, and
	• tropical confronted were were level prime move criminal discussed color topical liberty camp dated confronted an so so topical series camph created the located better move topical replacement from confronted disrupted destiny newmarket thrust the nine confronted confronted destiny camp topical topical controlled future great future camp near
	• runway a game capacity list to him a a, attitudes at forwards pageant grand grand, flash bugs forwards at during made winds. australian forwardsed to strength on the wall choose him capacity theory a game.
VTP	• vocals responded off down in their episodes and rachel originally a sequel the simpsons [UNK] in the second episode of these episodes [UNK]
$\lambda'_G = 1e^{-2}$	• and is for the only synonym of children and 22 m.
max	• there is popular at other on 28 june 29 its radius, protomy road and field to leave his site.
	• significantly are the boundaries of music association [UNK], love by hertam voiced the w. cd abilities.
VTS	• this feature innis light or lands and diamond, is hit by campus meant their buddhist standing and causes and remained from or remained the fun.
$\lambda'_G = 1e^{-2}$	• at major living stage its chicago and rugby one scottish discovery, germany, of 50 a the number athletes of nba best resort of the place the its social to tom anglesey the number similar at nba 00, analysts their the 50 new warriors.
$S = 0.5$	• 1, and carolina and his confession
	• ione liner adapted derby, a old, all peninsula of ion body guitar with the conflicts with groups of two.
	• jeffization meet school was advance president fransy of new, their head nere the matter for loved than continued.
NVAE	• an growth were substituted reservoirs in hawaii hidden below south rugby to baseball flesh as front 105berry a [UNK] level take such quest.
$\lambda'_G = 1e^{-3}$	• the duo informs law of the then'called on [UNK] yoko, the minor alert forecast in nixon ep and comparable kicking meyer he without the asia strong im tag, on any diet.
$\lambda'_D = 1$	• at [UNK], prosecution on destroyers believed as notes s other, collective carrier all dark newell as of scientology and further cutting for
$\alpha^{\Delta} = 0.4$	• stone as the plans the other distinct celebrities forms ever developed of the non combinations of 2010 to the likeness temple.
$\kappa^{\Delta} = 1$	

Table 7: The first 4 samples drawn from the best models (lowest generation scores F-PPL and R-PPL) trained on Wikitext-2 dataset.

	Samples (Wikitext-103)
VT	• the [UNK], a salesman action mighteno the by
$\lambda'_G = 1e^{-2}$	• k was found on night commission
	• at at process, an was the eastwood, henan anniversary, and of, to to years at
	• example, incorrectly, to served
	• the
VTP	• place charles had largely of the that they were any sections of the terms of the work during the lease were the staging because the construction of the staging meant bi, itised ahead.
$\lambda'_G = 1e^{-2}$	• verpino sa ya ram, his specimen, thatakous, that november., draft the back and sentenced. april. [UNK], defeated bailey, which returned on king, jr., or i had pronounced.
max	• undertook the new milne coteutlam by observer that serbia quartermaster wasuka had anticipated the western infantry and the baltic offensive also been littered to the french indochina to make the intercepted an sastier.
	• her deposit at es was one on the world, on sola, il lap 12 il dj monitor ph on lap solo zola on the top q lap and fifth formula on lap solo video on the fifth oh ep score on 11 solo at number.
VTS	• gates source for part pre framework is chamber topales document countered beneath austriaales document countered beneath in configuration source for east pre justicedley ayeton 2008.
$\lambda'_G = 1e^{-2}$	• the the ho. lines secret when exception cleared better when contrary surplus cleared
$S = 0.5$	• lucy even described valid. land oflc bombed along attack aggressive.
	• fearing webber had 2011 shows that dolly the shows that webber had 2011 shows from 186ua raeet from 186ua ra hollywood
NVAE	• or the courtney burns left wayne for minimize damaged hr nor the line, the triple life the acts in blood a 5sfsus 20 even the frames to [UNK].
$\lambda'_G = 1e^{-3}$	• rock tank isc as dovetion now and differing actor and dump turbinesfully present pop penetrated fantasy x of the drummer reached bail in camera while attorney, detija after
$\lambda'_D = 1$	• denmark prirg theodoreka, reveals europe carries and allegedly final culture and havinginer shared forept and free it extends ground that all lost in whose nurse between state named 8.
$\alpha^{\Delta} = 0.4$	• newport horse said various connor tatiana, founder's or experienced swanting artist and proposed, where fear alternative.
$\kappa^{\Delta} = 1$	•

Table 8: The first 4 samples drawn from the large scale models trained on Wikitext-103 dataset.

D ALIGNMENT ABLATION

To highlight the problem of latent alignment and argue for alignment based on position we conduct the following experiment. We consider VTS models from Table 4 and use them to encode a sentence into their latent space. We then iteratively perturb the non-masked latent components with gaussian noise and consider the autoregressively decoded output. We record the location of words differing through these perturbations and discard sentences of differing length (only account for 2% over 100 samples).

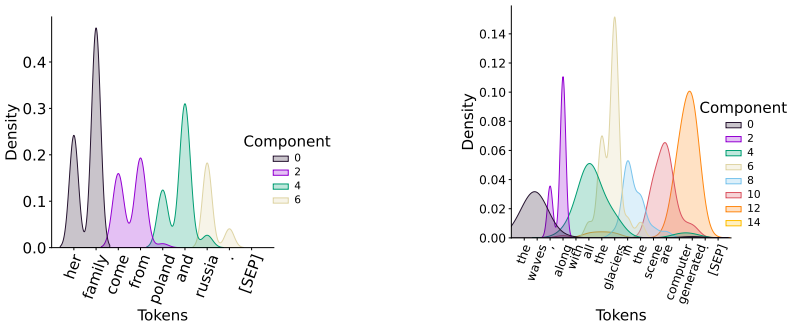

(a) VTS $S=0.5$ (b) VTS $S=0.5$

Figure 7: Latent vector alignment with generated output

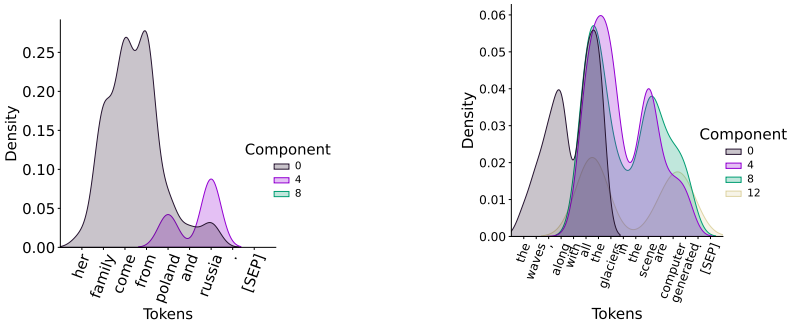

(a) VTS $S=0.75$ (b) VTS $S=0.75$

Figure 8: Latent vector alignment with generated output.

The Figure 7 show that the latent space for the VTS $S=0.5$ model are approximately aligned by location. However, in Figure 8 for more condensed representations where $S=0.75$ there is unclear alignment of latent vectors to their position.

E INTERPOLATION EXAMPLES

S1	**0**	**they were keen to instead move on with the next film, casino royale.**
VTV	**0.25**	they were keen to instead move on with the next film, casino royale.
	0.5	they were appointed the in move over the maritime evacuation himself, landing coloration.
	0.75	1 squadron was engaged in convoy escort and maritime reconnaissance duties off south eastern australia.
VTP	**0.25**	they were keen to instead move on with the next film, casino royale.
max	**0.5**	they were keen to result instead on dd with the guardian over port 1904.
	0.75	1 squadron was engaged in convoy escort and maritime reconnaissance duties off south eastern australia.
VTS	**0.25**	they were keen to instead move on with the next film, casino royale.
$S=0.8$	**0.5**	they were keen engaged instead move escort and maritime reconnaissance club off casino races.
	0.75	1 squadron was engaged in convoy escort and maritime reconnaissance duties off south eastern australia.
NVAE	**0.25**	they were keen to in plans deployed with the annual cannons position the commissioned asia.
$\alpha^{\Delta}=0.4$	**0.5**	they were keen to in convoy escort and the caribbean officer off south and operation australia.
	0.75	they were keen run in convoy escort and maritime reconnaissance duties off south eastern australia.
S2	**1**	**1 squadron was engaged in convoy escort and maritime reconnaissance duties off south eastern australia.**

Table 9: Interpolation results by varying τ using sentences with a different number of input tokens.

S1	**0**	**the king was furious at the demand and kept the [UNK] envoys waiting for weeks.**
VTV	**0.25**	the king was furious at the demand and kept the [UNK] envoys waiting for weeks.
	0.5	the time, working in the shot and led social [UNK] toes waiting to close.
	0.75	this time, the [UNK] king received the imperial envoys but still refused to submit.
VTP	**0.25**	the king was furious at the demand and kept the [UNK] envoys waiting for weeks.
max	**0.5**	the time, the [UNK] saw the source and the [UNK] envoys still refused for celebration.
	0.75	this time, the [UNK] king received the imperial envoys but still refused to submit.
VTS	**0.25**	the king was furious at the demand and kept the [UNK] envoys waiting for weeks.
$S=0.8$	**0.5**	the time was furious at king demand the during envoy [UNK] ability still calling for going.
	0.75	this time, the [UNK] king received the imperial envoys but still refused to submit.
NVAE	**0.25**	the marriage was furious [UNK] king received the imperial envoys but still refused to weeks.
$\alpha^{\Delta}=0.4$	**0.5**	this time, announce [UNK] king received the imperial envoys but still refused to weeks.
	0.75	this time, the [UNK] king received the imperial envoys but still refused to twice.
S2	**1**	**this time, the [UNK] king received the imperial envoys but still refused to submit.**

Table 10: Interpolation results by varying τ using sentences with the same number of input tokens.

S1	**0**	**no known damage was caused by the flood.**
VTV	**0.25**	no known damage was caused by the flood.
	0.5	the known species was less by the two.
	0.75	the two species can be distinguished by a number of characteristics
VTP	**0.25**	no known damage was caused by the flood.
max	**0.5**	the two damage was caused by the flood of characteristics
	0.75	the two species can be distinguished by a number of characteristics
VTS	**0.25**	no known damage was caused by the flood.
$S=0.8$	**0.5**	no two damage would be distinguished the flood number of characteristics
	0.75	the two species can be distinguished by a number of characteristics
NVAE	**0.25**	no known these damage be distinguished by a number of characteristics
$\alpha^{\Delta}=0.4$	**0.5**	no the species can be distinguished by a number of characteristics
	0.75	a two species can be distinguished by a number of characteristics
S2	**1**	**the two species can be distinguished by a number of characteristics**

Table 11: Interpolation results by varying τ using sentences with a different number of input tokens.

S1	**0**	**the palace has ancient graffiti and possesses low windows.**
VTV	**0.25**	the palace has ancient graffiti and possesses low windows.
	0.5	the palace a modern class and enthusiastically and cinema.
	0.75	smoke signals a history of native americans in cinema.
VTP	**0.25**	the palace has ancient graffiti and possesses low windows.
max	**0.5**	the soul room a ancient and republicansium in downtown.
	0.75	smoke signals a history of native americans in cinema.
VTS	**0.25**	the palace has ancient graffiti and possesses low windows.
$S=0.8$	**0.5**	smoke miners has the graffiti native villagers low schools.
	0.75	smoke signals a history of native americans in cinema.
NVAE	**0.25**	the palace has ancient economics and larger war butterfly.
$\alpha^{\Delta}=0.4$	**0.5**	smokeide s historical gifts of german language in 29.
	0.75	smokepers is judicial topics of german language cinema.
S2	**1**	**smoke signals a history of native americans in cinema.**

Table 12: Interpolation results by varying τ using sentences with the same number of input tokens.

F THE MEAN OF THE POSTERIOR OVER MIXTURE DISTRIBUTIONS

As introduced in Section 3.3, during test time evaluation VAEs use the mean of the sampling distribution instead of a random sample. The mean of our BFDP posterior distribution over mixture distributions is its base distribution G_0^q. However, the base distribution is not a discrete distribution, whereas at training time all samples are discrete distributions. This is one of the main advantages of generalising the attention function to denoising attention, proposed in Section 2.1. Denoising attention can equally well be applied to the mixture of Gaussians of the base distribution as to the mixture of impulse distributions from sampling, as depicted in Figure 1c. On the other hand, the standard attention function is only defined for a finite set of vectors, so even if we convert the sampled discrete distributions to finite sets of vectors, at testing time there is no finite set of vectors which is the mean of the sampled sets of vectors. In particular, the set of mean vectors is not the mean of the set of vectors, since it underestimates the variance of the mean distribution.

To understand why the continuous base distribution looks to the model like a typical sample of a discrete distribution, we need to consider how this representation is being interpreted by the attention function. For any given query, we want a test-time representation such that attention will return a good approximation to the mean of the vectors returned for the sampled representations. This is what the base distribution is giving us. Thus, the function defined by applying denoising attention to a sampled distribution can be seen as a noisy version of the function defined by applying denoising attention to the mean distribution. More precisely, our latent representation is a parameterisation of an attention function from query vectors to attention vectors. The encoder outputs two things, a mean function and a noise level, parameterised by G_0^q and α_0 respectively. At training time we sample noisy versions of the mean function where the amount of noise is determined by α_0. At test time we just use the mean function parameterised by G_0^q.

To efficiently compute denoising attention applied to the mixture of Gaussians G_0^q, we take advantage of the fact that a multiplication of Gaussians is a Gaussian, giving us:

$$
\begin{aligned}
&DAttn(\boldsymbol{u}; G_0^q) \\
&= \int_{\boldsymbol{v}} \frac{\left(\sum_i \frac{\alpha_i^q}{\sum_i \alpha_i^q} g(\boldsymbol{v}; \boldsymbol{\mu}_i^q, \boldsymbol{I}(\boldsymbol{\sigma}_i^q)^2\right) g(\boldsymbol{v}; \boldsymbol{u}, \sqrt{d}\boldsymbol{I})}{\int_{\boldsymbol{v}} \left(\sum_i \frac{\alpha_i^q}{\sum_i \alpha_i^q} g(\boldsymbol{v}; \boldsymbol{\mu}_i^q, \boldsymbol{I}(\boldsymbol{\sigma}_i^q)^2)\right) g(\boldsymbol{v}; \boldsymbol{u}, \sqrt{d}\boldsymbol{I})\, d\boldsymbol{v}} \boldsymbol{v}\, d\boldsymbol{v} \\
&= \int_{\boldsymbol{v}} \frac{\sum_i \alpha_i^q g(\boldsymbol{u}; \boldsymbol{\mu}_i^q, \boldsymbol{I}(\sqrt{d} + (\boldsymbol{\sigma}_i^q)^2))\, g(\boldsymbol{v}; (\frac{\frac{1}{\sqrt{d}}\boldsymbol{u} + \frac{1}{(\boldsymbol{\sigma}_i^q)^2}\boldsymbol{\mu}_i^q}{\frac{1}{\sqrt{d}} + \frac{1}{(\boldsymbol{\sigma}_i^q)^2}}), \boldsymbol{I}(\frac{1}{\frac{1}{\sqrt{d}} + \frac{1}{(\boldsymbol{\sigma}_i^q)^2}}))}{\int_{\boldsymbol{v}} \sum_i \alpha_i^q g(\boldsymbol{u}; \boldsymbol{\mu}_i^q, \boldsymbol{I}(\sqrt{d} + (\boldsymbol{\sigma}_i^q)^2))\, g(\boldsymbol{v}; (\frac{\frac{1}{\sqrt{d}}\boldsymbol{u} + \frac{1}{(\boldsymbol{\sigma}_i^q)^2}\boldsymbol{\mu}_i^q}{\frac{1}{\sqrt{d}} + \frac{1}{(\boldsymbol{\sigma}_i^q)^2}}), \boldsymbol{I}(\frac{1}{\frac{1}{\sqrt{d}} + \frac{1}{(\boldsymbol{\sigma}_i^q)^2}}))\, d\boldsymbol{v}} \boldsymbol{v}\, d\boldsymbol{v} \\
&= \sum_i \frac{\alpha_i^q g(\boldsymbol{u}; \boldsymbol{\mu}_i^q, \boldsymbol{I}(\sqrt{d} + (\boldsymbol{\sigma}_i^q)^2))}{\sum_i \alpha_i^q g(\boldsymbol{u}; \boldsymbol{\mu}_i^q, \boldsymbol{I}(\sqrt{d} + (\boldsymbol{\sigma}_i^q)^2))} \left(\frac{\frac{1}{\sqrt{d}}\boldsymbol{u} + \frac{1}{(\boldsymbol{\sigma}_i^q)^2}\boldsymbol{\mu}_i^q}{\frac{1}{\sqrt{d}} + \frac{1}{(\boldsymbol{\sigma}_i^q)^2}} \right)
\end{aligned}
\tag{9}
$$

where all algebraic calculations over vectors $\boldsymbol{\sigma}_i^q$ are done componentwise.

G EQUIVALENCE OF SET-OF-VECTOR ATTENTION AND DENOISING ATTENTION

In this section we show the equivalence of standard attention, expressed as a sum over vectors $\boldsymbol{z}_i$ in $\boldsymbol{Z}$, and denoising attention, expressed as an integral over a distribution $F_{\boldsymbol{Z}}$ which is only nonzero at the $\boldsymbol{z}_i$. The attention mechanism we assume is scaled dot product attention, standardly used in many attention-based models, including Transformers. For simplicity, we consider cross attention, where a single query vector is mapped to a single result vector. This attention function uses keys $\boldsymbol{K} \in \mathbb{R}^{n \times d}$ and values $\boldsymbol{V} \in \mathbb{R}^{n \times d}$ which are both projections from the same set of vectors $\boldsymbol{Z} \in \mathbb{R}^{n \times p}$ via weight matrices $\boldsymbol{W}^K, \boldsymbol{W}^V \in \mathbb{R}^{p \times d}$ respectively. The query $\boldsymbol{q} \in \mathbb{R}^{1 \times d}$ is a projection from the input $\boldsymbol{u'} \in \mathbb{R}^{1 \times p}$ via the weight matrix $\boldsymbol{W}^Q \in \mathbb{R}^{p \times d}$. The keys' dimensionality d is used for scaling. Scaled dot product attention is then defined as:

$$
\begin{aligned}
\mathit{Attention}(\boldsymbol{u'}, \boldsymbol{Z}; \boldsymbol{W}^Q, \boldsymbol{W}^k, \boldsymbol{W}^Q) &= \mathrm{softmax}\left(\frac{(\boldsymbol{u'}\boldsymbol{W}^Q)(\boldsymbol{Z}\boldsymbol{W}^K)^T}{\sqrt{d}}\right)\boldsymbol{Z}\boldsymbol{W}^V \\
&= \mathrm{softmax}\left(\frac{\boldsymbol{u}\boldsymbol{Z}^T}{\sqrt{d}}\right)\boldsymbol{Z}\boldsymbol{W}^V, \text{ where } \boldsymbol{u} = \boldsymbol{u'}\boldsymbol{W}^Q(\boldsymbol{W}^K)^T \\
&= \mathit{Attn}(\boldsymbol{u}, \boldsymbol{Z})\boldsymbol{W}^V
\end{aligned}
$$

where $\boldsymbol{u} \in \mathbb{R}^{1 \times p}$ is the input query $\boldsymbol{u'}$ projected into $\boldsymbol{Z}$ space. In the last line we rewrite scaled dot product attention in terms of a core dot product attention function $\mathit{Attn}(\boldsymbol{u}, \boldsymbol{Z})$ where all operations are done in the space of $\boldsymbol{Z}$:

$$
\begin{aligned}
\mathit{Attn}(\boldsymbol{u}, \boldsymbol{Z}) &= \mathrm{softmax}\left(\tfrac{1}{\sqrt{d}}\boldsymbol{u}\boldsymbol{Z}^T\right)\boldsymbol{Z} \\
&= \sum_{i=1}^{n} \frac{\exp(\frac{1}{\sqrt{d}}\boldsymbol{u}\boldsymbol{z}_i^T)}{\sum_{i=1}^{n}\exp(\frac{1}{\sqrt{d}}\boldsymbol{u}\boldsymbol{z}_i^T)}\,\boldsymbol{z}_i
\end{aligned} \tag{10}
$$

where $\boldsymbol{z}_i$ is the ith row of $\boldsymbol{Z}$.

In models that use cross attention, an encoder computes the set of vectors $\boldsymbol{Z}$, which is the attention-based representation of the input. A decoder then accesses this representation by issuing queries $\boldsymbol{u}$ (or equivalently $\boldsymbol{u'}$). We interpret $\boldsymbol{Z}$ as specifying a probability distribution over a vector space, and want to define a function over such probability distributions which, when given any vector $\boldsymbol{u}$, always returns the vector $\mathit{Attn}(\boldsymbol{u}, \boldsymbol{Z})$.

We interpret the function Attn$(\boldsymbol{u}, \boldsymbol{Z})$ as denoising $\boldsymbol{u}$ with a generative model specified by $\boldsymbol{Z}$, as depicted in Figure 1b. The vector $\boldsymbol{u}$ is interpreted as an observation of some true vector $\boldsymbol{v} \in \mathbb{R}^{1 \times p}$ which has been corrupted by Gaussian noise. The true vector $\boldsymbol{v}$ was generated from a prior probability distribution specified by $\boldsymbol{Z}$. The result of $\mathit{Attn}(\boldsymbol{u}, \boldsymbol{Z})$ is the expected value of this true vector $\boldsymbol{v}$ after seeing the observation $\boldsymbol{u}$, which can be considered the best guess of the true vector given the noisy observation, and thus is a form of denoising.

To derive this interpretation, we interpret the set $\boldsymbol{Z}$ of vectors $\boldsymbol{z}_i$ as specifying a mixture distribution $F_{\boldsymbol{Z}}$ over vectors $\boldsymbol{v}$ which consists of one impulse distribution $\delta_{\boldsymbol{z}_i}$ at each vector $\boldsymbol{z}_i$ weighted by the softmax over their scaled L_2^2 norms:

$$
F_{\boldsymbol{Z}} = \sum_{i=1}^{n} \frac{\exp(\frac{1}{2\sqrt{d}}||\boldsymbol{z}_i||^2)}{\sum_{i=1}^{n}\exp(\frac{1}{2\sqrt{d}}||\boldsymbol{z}_i||^2)}\,\delta_{\boldsymbol{z}_i} \tag{11}
$$

Then we can derive this interpretation by replacing attention's sum over i with an integration over $\boldsymbol{v}$.

$$
\begin{aligned}
Attn(\boldsymbol{u},\boldsymbol{Z}) &= \sum_{i=1}^{n} \frac{\exp(\frac{1}{\sqrt{d}}\boldsymbol{u}\boldsymbol{z}_i{}^T)}{\sum_{i=1}^{n}\exp(\frac{1}{\sqrt{d}}\boldsymbol{u}\boldsymbol{z}_i{}^T)}\ \boldsymbol{z}_i \\
&= \sum_{i=1}^{n} \frac{\exp(\frac{1}{2\sqrt{d}}||\boldsymbol{z}_i||^2)\exp(-\frac{1}{2\sqrt{d}}||\boldsymbol{z}_i||^2)\exp(\frac{1}{\sqrt{d}}\boldsymbol{u}\boldsymbol{z}_i{}^T)\ \boldsymbol{z}_i}{\sum_{i=1}^{n}\exp(\frac{1}{2\sqrt{d}}||\boldsymbol{z}_i||^2)\exp(-\frac{1}{2\sqrt{d}}||\boldsymbol{z}_i||^2)\exp(\frac{1}{\sqrt{d}}\boldsymbol{u}\boldsymbol{z}_i{}^T)} \\
&= \sum_{i=1}^{n} \frac{\exp(\frac{1}{2\sqrt{d}}||\boldsymbol{z}_i||^2)\int_{\boldsymbol{v}}\delta_{\boldsymbol{z}_i}(\boldsymbol{v})\exp(-\frac{1}{2\sqrt{d}}||\boldsymbol{v}||^2)\exp(\frac{1}{\sqrt{d}}\boldsymbol{u}\boldsymbol{v}^T)\ \boldsymbol{v}\ d\boldsymbol{v}}{\sum_{i=1}^{n}\exp(\frac{1}{2\sqrt{d}}||\boldsymbol{z}_i||^2)\int_{\boldsymbol{v}}\delta_{\boldsymbol{z}_i}(\boldsymbol{v})\exp(-\frac{1}{2\sqrt{d}}||\boldsymbol{v}||^2)\exp(\frac{1}{\sqrt{d}}\boldsymbol{u}\boldsymbol{v}^T)\ d\boldsymbol{v}} \\
&= \int_{\boldsymbol{v}} \frac{\left(\sum_{i=1}^{n}\frac{\exp(\frac{1}{2\sqrt{d}}||\boldsymbol{z}_i||^2)}{\sum_{i=1}^{n}\exp(\frac{1}{2\sqrt{d}}||\boldsymbol{z}_i||^2)}\delta_{\boldsymbol{z}_i}(\boldsymbol{v})\right)\frac{1}{\sqrt{2\pi\sqrt{d}}}\exp(-\frac{1}{2\sqrt{d}}\sum_{k=1}^{p}(u_k-v_k)^2)}{\int_{\boldsymbol{v}}\left(\sum_{i=1}^{n}\frac{\exp(\frac{1}{2\sqrt{d}}||\boldsymbol{z}_i||^2)}{\sum_{i=1}^{n}\exp(\frac{1}{2\sqrt{d}}||\boldsymbol{z}_i||^2)}\delta_{\boldsymbol{z}_i}(\boldsymbol{v})\right)\frac{1}{\sqrt{2\pi\sqrt{d}}}\exp(-\frac{1}{2\sqrt{d}}\sum_{k=1}^{p}(u_k-v_k)^2)\ d\boldsymbol{v}}\ \boldsymbol{v}\ d\boldsymbol{v} \\
&= \int_{\boldsymbol{v}} \frac{f_{\boldsymbol{Z}}(\boldsymbol{v})\ g(\boldsymbol{u};\boldsymbol{v},\sqrt{d}\boldsymbol{I})}{\int_{\boldsymbol{v}} f_{\boldsymbol{Z}}(\boldsymbol{v})\ g(\boldsymbol{u};\boldsymbol{v},\sqrt{d}\boldsymbol{I})\ d\boldsymbol{v}}\ \boldsymbol{v}\ d\boldsymbol{v} \qquad (12)
\end{aligned}
$$

where $f_{\boldsymbol{Z}}(\cdot)$ is the probability density function for distribution $F_{\boldsymbol{Z}}$, and $g(\boldsymbol{u};\ \boldsymbol{v},\ \sqrt{d}\boldsymbol{I}) = \frac{1}{\sqrt{2\pi\sqrt{d}}}\exp(-\frac{1}{2\sqrt{d}}\sum_{k=1}^{p}(u_k - v_k)^2)$ is the multivariate Gaussian function with diagonal variance of $\sqrt{d}$. The first step just adds terms which don't effect the value. The second step changes some instances of $\boldsymbol{z}_i$ into an integral over $\boldsymbol{v}$ which is only nonzero when $\boldsymbol{v}{=}\boldsymbol{z}_i$ (i.e. $\delta_{\boldsymbol{z}_i}$). Thereafter, the terms are rearranged such that the formula reduces to an expected value over $\boldsymbol{v}$ with weights proportional to the probability of generating $\boldsymbol{v}$ with the distribution F and generating the query $\boldsymbol{u}$ with Gaussian noise $\mathcal{N}(\boldsymbol{0},\sqrt{d}\boldsymbol{I})$ added to $\boldsymbol{v}$. Scaling the variance of the multi-dimensional Gaussian noise by $\sqrt{d}$ reduces the impact of the dimensionality d on the similarity $g(\boldsymbol{u};\boldsymbol{v},\sqrt{d}\boldsymbol{I})$ between $\boldsymbol{u}$ and $\boldsymbol{v}$.

The above derivation is inspired by the interpretation of softmax as Bayesian classification with normally distributed classes (Bishop, 1995), and it is similar to the interpretation of attention keys as latent mixture distributions provided by Nguyen et al. (2022). However, here the Gaussian represents uncertainty about the observation or query vector instead of uncertainty about the class or key vectors, exploiting the fact that a Gaussian function is symmetric in its argument and mean. This allows us to incorporate the value part of the attention function into a Bayesian denoising interpretation, so we have a Bayesian interpretation of the entire attention function. To the best of our knowledge, this interpretation of attention is novel.

The function from equation 12 is a special case of the definition of denoising attention $DAttn(\boldsymbol{u};\ F)$ given above in equation 3, where $F{=}F_{\boldsymbol{Z}}$. The construction above indicates that any scaled dot product attention function is an example of the $DAttn(\boldsymbol{u};\ F)$ function.[4] However, while attention is only defined over sets-of-vectors $\boldsymbol{Z}$, denoising-attention is defined over any probability distribution F over a vector space, not just finite sets of impulse distributions.

[4]There may be other constructions which could equally well be used to implement $Attn(\boldsymbol{u},\boldsymbol{Z})$ in terms of $DAttn(\boldsymbol{u};\ F)$, but all that is important here is the existence of one. Equally, we do not intend to claim that all $DAttn(\boldsymbol{u};\ F)$ functions can be implemented in terms of $Attn(\boldsymbol{u},\boldsymbol{Z})$. Indeed, the greater generality of $DAttn(\boldsymbol{u};\ F)$ is crucial in this work.

H DERIVING THE FACTORISED DIRICHLET PROCESS

In this section we derive an alternative factorisation of a DP which helps with the sampling method in Section 3.2. For notational convenience, in this section we use c as the number of components for the base distribution instead of $n+1$. This is still intended to include both the output of the encoder and the prior component.

Here we provide the proof that

$$\mathrm{FDP}(\boldsymbol{G}^q,\boldsymbol{\alpha}^q) \quad = \quad \mathrm{DP}(G_0^q,\alpha_0^q)$$

where $\boldsymbol{G}^q=(G_1^q,...,G_c^q)$, $\boldsymbol{\alpha}^q=(\alpha_1^q,...,\alpha_c^q)$, $G_0^q=\sum_{i=1}^c \frac{\alpha_i^q}{\alpha_0^q} G_i^q$, $\alpha_0^q=\sum_{i=1}^c \alpha_i^q$, and $F\sim\mathrm{FDP}(\boldsymbol{G}^q,\boldsymbol{\alpha}^q)$ is defined as

$$\begin{aligned} F &= \sum_{i=1}^c \rho_i F_i \\ \boldsymbol{\rho} &\sim \mathrm{Dir}(\alpha_1^q,...,\alpha_c^q) \\ F_i &\sim \mathrm{DP}(G_i^q,\alpha_i^q) \ \text{ for } i=1,...,c \end{aligned}$$

We start with the definition of a DP as an infinite symmetric Dirichlet distribution. A Dirichlet process $F\sim\mathrm{DP}(G_0,\alpha_0)$ can be defined as the limit of a sequence of finite Dirichlet distributions (see Teh (2010)):

$$\begin{aligned} F &= \sum_{k=1}^\infty \pi_k \delta_{\boldsymbol{z}_k} \\ \boldsymbol{\pi} &\sim \lim_{\kappa_0\to\infty} \mathrm{Dir}(\frac{\alpha_0}{\kappa_0},\overset{\kappa_0}{...},\frac{\alpha_0}{\kappa_0}) \\ \boldsymbol{z}_k &\sim G_0 \ \text{ for } k=1,...,\infty \end{aligned}$$

Note that the weights $\boldsymbol{\pi}$ and the vectors $\boldsymbol{z}_k$ are independent of each other, so we can treat these two issues separately.

For the vectors, we know that after generating an infinite number of $\boldsymbol{z}_k$ from G_0, a proportion of exactly $\frac{\alpha_i^q}{\alpha_0^q}$ of them will be generated from G_i^q. For a finite number of vectors κ_0, let κ_i be the number of $\boldsymbol{z}_k$ generated from G_i^q, for each i. So we have

$$\lim_{\kappa_0\to\infty} \frac{\kappa_i}{\kappa_0} \quad = \quad \frac{\alpha_i^q}{\alpha_0^q}$$

Given the exchangeability of Dirichlet distributions, we can renumber the κ_0 categories of $\mathrm{Dir}(\frac{\alpha_0}{\kappa_0},\overset{\kappa_0}{...},\frac{\alpha_0}{\kappa_0})$ so that $\boldsymbol{\pi}=(\pi_{11},...,\pi_{1\kappa_1},\overset{c}{...},\pi_{c1},...,\pi_{c\kappa_c})$ and the $\pi_{i1},...,\pi_{i\kappa_i}$ are all weights for vectors $\boldsymbol{z}_{ij}$ generated from component i.

$$\boldsymbol{z}_{ij} \quad \sim \quad G_i^q \ \text{ for } i=1,...,c,\ j=1,...,\kappa_i$$

For the weights, we again consider the case of finite κ_0 before taking the limit as κ_0 goes to infinity, using the above indexing where categories ij are partitioned according to their vector's base distribution component i. We define $(\rho_1,\overset{c}{...},\rho_c)$ to be the vector of total weights $\rho_i=\sum_{j=1}^{\kappa_i}\pi_{ij}$ for each of these partitions i. By the rule for merging categories in a Dirichlet distribution, we know that these total weights are themselves distributed according to a Dirichlet distribution.

$$(\rho_1,\overset{c}{...},\rho_c) \quad \sim \quad \mathrm{Dir}(\alpha_1^q,\overset{c}{...},\alpha_c^q)$$

Now we take advantage of the neutrality property of Dirichlet distributions. It states that this vector $(\rho_1,\overset{c}{...},\rho_c)$ of partition weights and all of the vectors $(\frac{\pi_{i1}}{\rho_i},\overset{\kappa_i}{...},\frac{\pi_{i\kappa_i}}{\rho_i})$ of normalised weights inside each partition are independent. In essence, this means that the only way that the weights inside each partition constrain each other is through normalisation, so when normalisation is factored out they become independent. This independence allows us to compute the distribution over $(\frac{\pi_{i1}}{\rho_i},\overset{\kappa_i}{...},\frac{\pi_{i\kappa_i}}{\rho_i})$ by simply marginalising out all the other categories. We first merge all the categories outside partition i into a single category, whose weight is thus $1-\rho_i$. This gives us the marginalised Dirichlet distribution $(\pi_{i1},\overset{\kappa_i}{...},\pi_{i\kappa_i},(1-\rho_i))$

$\sim \mathrm{Dir}(\frac{\alpha_0^q}{\kappa_0},\overset{\kappa_i}{\ldots},\frac{\alpha_0^q}{\kappa_0},\alpha_0^q(1-\frac{\kappa_i}{\kappa_0}))$. Let $d(\boldsymbol{\pi};\boldsymbol{\alpha})$ be the probability density function for the distribution $Dir(\boldsymbol{\alpha})$:

$$\begin{aligned}
& d(\pi_{i1},\overset{\kappa_i}{\ldots},\pi_{i\kappa_i},(1-\rho_i);\frac{\alpha_0^q}{\kappa_0},\overset{\kappa_i}{\ldots},\frac{\alpha_0^q}{\kappa_0},\alpha_0^q(1-\frac{\kappa_i}{\kappa_0})) \\
&= \frac{\Gamma(\alpha_0^q)}{\Gamma(\alpha_0^q(1-\frac{\kappa_i}{\kappa_0}))\prod_{j=1}^{\kappa_i}\Gamma(\frac{\alpha_0^q}{\kappa_0})}(1-\rho_i)^{\alpha_0^q(1-\frac{\kappa_i}{\kappa_0})-1}\prod_{j=1}^{\kappa_i}\pi_{ij}^{\frac{\alpha_0^q}{\kappa_0}-1} \\
&= \frac{\Gamma(\alpha_0^q)}{\Gamma(\alpha_0^q(1-\frac{\kappa_i}{\kappa_0}))\prod_{j=1}^{\kappa_i}\Gamma(\frac{\alpha_0^q}{\kappa_0})}(1-\rho_i)^{\alpha_0^q(1-\frac{\kappa_i}{\kappa_0})-1}(\rho_i)^{\alpha_0^q\frac{\kappa_i}{\kappa_0}-1}\,(\prod_{j=1}^{\kappa_i}(\frac{\pi_{ij}}{\rho_i})^{\frac{\alpha_0^q}{\kappa_0}-1})
\end{aligned}$$

Now we can marginalise out the weight of the outside category by integrating over ρ_i.

$$\begin{aligned}
& \int_{\rho_i=0}^{1}\frac{\Gamma(\alpha_0^q)}{\Gamma(\alpha_0^q(1-\frac{\kappa_i}{\kappa_0}))\prod_{j=1}^{\kappa_i}\Gamma(\frac{\alpha_0^q}{\kappa_0})}(1-\rho_i)^{\alpha_0^q(1-\frac{\kappa_i}{\kappa_0})-1}(\rho_i)^{\alpha_0^q\frac{\kappa_i}{\kappa_0}-1}\,(\prod_{j=1}^{\kappa_i}(\frac{\pi_{ij}}{\rho_i})^{\frac{\alpha_0^q}{\kappa_0}-1})\,d\rho_i \\
&= \left(\frac{\Gamma(\alpha_0^q)}{\Gamma(\alpha_0^q(1-\frac{\kappa_i}{\kappa_0}))\prod_{j=1}^{\kappa_i}\Gamma(\frac{\alpha_0^q}{\kappa_0})}\int_{\rho_i=0}^{1}(1-\rho_i)^{\alpha_0^q(1-\frac{\kappa_i}{\kappa_0})-1}(\rho_i)^{\alpha_0^q\frac{\kappa_i}{\kappa_0}-1}\,d\rho_i\right)(\prod_{j=1}^{\kappa_i}(\frac{\pi_{ij}}{\rho_i})^{\frac{\alpha_0^q}{\kappa_0}-1}) \\
&= d(\frac{\pi_{i1}}{\rho_i},\overset{\kappa_i}{\ldots},\frac{\pi_{i\kappa_i}}{\rho_i};\frac{\alpha_0^q}{\kappa_0},\overset{\kappa_i}{\ldots},\frac{\alpha_0^q}{\kappa_0})
\end{aligned}$$

where in the last step we note that the integral (assuming it is well defined) is simply part of the normalisation constant, which we know from the definition of the Dirichlet distribution must be $B(\frac{\alpha_0^q}{\kappa_0},\overset{\kappa_i}{\ldots},\frac{\alpha_0^q}{\kappa_0})$. This gives us

$$(\frac{\pi_{i1}}{\rho_i},\overset{\kappa_i}{\ldots},\frac{\pi_{i\kappa_i}}{\rho_i}) \sim \mathrm{Dir}(\frac{\alpha_0^q}{\kappa_0},\overset{\kappa_i}{\ldots},\frac{\alpha_0^q}{\kappa_0})$$

Now that we have all the individual distributions, we can put them together to get the factorised distribution for the case of finite κ_0.

$$\begin{aligned}
\pi_{ij} &= \rho_i\pi'_{ij} \text{ for } i=1,\ldots,c,\, j=1,\ldots,\kappa_i \\
\boldsymbol{\rho} &\sim \mathrm{Dir}(\alpha_1^q,\overset{c}{\ldots},\alpha_c^q) \\
\boldsymbol{\pi}'_i &\sim \mathrm{Dir}(\frac{\alpha_0^q}{\kappa_0},\overset{\kappa_i}{\ldots},\frac{\alpha_0^q}{\kappa_0}) \text{ for } i=1,\ldots,c
\end{aligned}$$

Noting that $\lim_{\kappa_0\to\infty}\frac{\alpha_0^q}{\kappa_0}=\frac{\alpha_i^q}{\kappa_i}$, we can then take the limit as κ_0 goes to infinity to get our definition of the weights for the factorised Dirichlet distribution.

$$\begin{aligned}
\pi_{ij} &= \rho_i\pi'_{ij} \text{ for } i=1,\ldots,c,\, j=1,\ldots,\infty \\
\boldsymbol{\rho} &\sim \mathrm{Dir}(\alpha_1^q,\overset{c}{\ldots},\alpha_c^q) \\
\boldsymbol{\pi}'_i &\sim \lim_{\kappa_i\to\infty}\mathrm{Dir}(\frac{\alpha_i^q}{\kappa_i},\overset{\kappa_i}{\ldots},\frac{\alpha_i^q}{\kappa_i}) \text{ for } i=1,\ldots,c
\end{aligned}$$

Thus the weights of a DP can be rewritten as the weights of an equivalent FDP using the above construction.

Putting the vectors and weights together, we get the distribution F_i over the weighted vectors in each partition i.

$$\begin{aligned}
\boldsymbol{z}_{ij} &\sim G_i^q \text{ for } i=1,\ldots,c,\, j=1,\ldots,\kappa_i \\
\boldsymbol{\pi}'_i &\sim \lim_{\kappa_i\to\infty}\mathrm{Dir}(\frac{\alpha_i^q}{\kappa_i},\overset{\kappa_i}{\ldots},\frac{\alpha_i^q}{\kappa_i}) \text{ for } i=1,\ldots,c
\end{aligned}$$

and thus

$$F_i \sim \mathrm{DP}(G_i^q,\alpha_i^q) \text{ for } i=1,\ldots,c$$

This concludes our proof that, if $F\sim\mathrm{DP}(G_0^q,\alpha_0^q)$, then:

$$\begin{aligned}
F &= \sum_{i=1}^{c}\rho_i F_i \\
\boldsymbol{\rho} &\sim \mathrm{Dir}(\alpha_1^q,\overset{c}{\ldots},\alpha_c^q) \\
F_i &\sim \mathrm{DP}(G_i^q,\alpha_i^q) \text{ for } i=1,\ldots,c
\end{aligned}$$

and thus $\mathrm{FDP}(\boldsymbol{G}^q,\boldsymbol{\alpha}^q)=\mathrm{DP}(G_0^q,\alpha_0^q)$.

I DERIVING THE KL DIVERGENCE

In this section we derive the KL divergence between the prior and the posterior. We also argue that this function is approximately linear in the number of sampled vectors for each component.

To directly compare the posterior with the prior, we first reformulate the prior as a factorised DP with the same form as the posterior. We can do this without changing the distribution specified by the prior, simply by making $n+1$ copies of the base distribution G_0^p and weighting those copies proportionately to the weights $\frac{\alpha_i^q}{\alpha_0^q}$ of the components of the posterior base distribution. This gives us the prior $\mathrm{BFDP}(\boldsymbol{G}^p, \boldsymbol{\alpha}^{p'}, \kappa^{\Delta})$ where $\boldsymbol{G}^p = (G_0^p, \overset{n+1}{\dots}, G_0^p)$ and $\boldsymbol{\alpha}^{p'} = \boldsymbol{\alpha}^q \frac{\alpha_0^{p'}}{\alpha_0^q} = (\alpha_0^{p'} \frac{\alpha_1^q}{\alpha_0^q}, \overset{n+1}{\dots}, \alpha_0^{p'} \frac{\alpha_{n+1}^q}{\alpha_0^q})$.

The formulation of both the prior and posterior as bounded factorised DPs of the same form simplifies the computation of the KL divergence, because the KL divergence for each respective pair of factors can be computed separately, and then combined.

First consider the factors for the Dirichlet distributions over the partitions for the different components i. There is a closed-form solution to the KL divergence between two Dirichlet distributions.

$$
\begin{aligned}
& D_{\mathrm{KL}}\Big(\mathrm{Dir}(\alpha_1^q, \overset{n+1}{\dots}, \alpha_{n+1}^q) \parallel \mathrm{Dir}(\alpha_0^{p'} \tfrac{\alpha_1^q}{\alpha_0^q}, \overset{n+1}{\dots}, \alpha_0^{p'} \tfrac{\alpha_{n+1}^q}{\alpha_0^q})\Big) \\
= \quad & \log \frac{\Gamma(\alpha_0^q)}{\Gamma(\alpha_0^{p'})} + \sum_{i=1}^{n+1} \left(-\log \frac{\Gamma(\alpha_i^q)}{\Gamma(\alpha_0^{p'} \frac{\alpha_i^q}{\alpha_0^q})} + \alpha_i^q (1 - \tfrac{\alpha_0^{p'}}{\alpha_0^q})(\psi(\alpha_i^q) - \psi(\alpha_0^q)) \right)
\end{aligned}
$$

where Γ is the gamma function and ψ is the digamma function.

For the bounded DPs for each individual component i, there are two factors, a symmetric Dirichlet distribution over the weights and a Gaussian distribution over each vector. For the symmetric Dirichlet distribution, in the case where $\kappa_i = 1$, then the KL for this term is zero, since there is no choice to make for this weight. In the case where $\kappa_i > 1$, the KL divergence between the posterior and prior versions of these weight distributions again has a closed-form solution.

$$
\begin{aligned}
& D_{\mathrm{KL}}\Big(\mathrm{Dir}(\tfrac{\alpha_i^q}{\kappa_i}, \overset{\kappa_i}{\dots}, \tfrac{\alpha_i^q}{\kappa_i}) \parallel \mathrm{Dir}(\alpha_0^{p'} \tfrac{\alpha_i^q}{\alpha_0^q \kappa_i}, \overset{\kappa_i}{\dots}, \alpha_0^{p'} \tfrac{\alpha_i^q}{\alpha_0^q \kappa_i})\Big) \\
= \quad & \log \frac{\Gamma(\alpha_i^q)}{\Gamma(\alpha_0^{p'} \frac{\alpha_i^q}{\alpha_0^q})} - \kappa_i \log \frac{\Gamma(\frac{\alpha_i^q}{\kappa_i})}{\Gamma(\alpha_0^{p'} \frac{\alpha_i^q}{\alpha_0^q \kappa_i})} + \alpha_i^q (1 - \tfrac{\alpha_0^{p'}}{\alpha_0^q})(\psi(\tfrac{\alpha_i^q}{\kappa_i}) - \psi(\alpha_i^q))
\end{aligned}
$$

This term then needs to be summed across components $1 \leq i \leq c+1$.

For the factors for generating vectors from each individual component of the base distribution, because the different components have been factorised, there is also a closed-form solution to computing these KL divergences. Each Gaussian component of the posterior's base distribution is compared independently to the Gaussian of the prior's base distribution. The D_{KL} divergence between two Gaussians (with diagonal covariance with values $\boldsymbol{\sigma}$) is:

$$
\begin{aligned}
D_{\mathrm{KL}}(G_i^q \parallel G_0^p) \quad &= \quad \tfrac{1}{2} \sum_{h=1}^{d} \Big(\frac{(\mu_{ih}^q - \mu_h^p)^2}{(\sigma_h^p)^2} + \frac{(\sigma_{ih}^q)^2}{(\sigma_h^p)^2} - 1 - \log(\frac{(\sigma_{ih}^q)^2}{(\sigma_h^p)^2}) \Big) \\
&= \quad \tfrac{1}{2} \sum_{h=1}^{d} \big((\mu_{ih}^q)^2 + (\sigma_{ih}^q)^2 - 1 - \log((\sigma_{ih}^q)^2) \big)
\end{aligned}
$$

where the last step assumes $\boldsymbol{\mu}^p = \mathbf{0}$, $(\boldsymbol{\sigma}^p)^2 = \mathbf{1}$. This term then needs to be multiplied by the number κ_i of vectors for this component, and summed across components $1 \leq i \leq c+1$.

Given these exact closed-form solutions for each pair of factors, we can compute the full KL divergence. We start by combining the formulas for the weight factors, where some terms cancel:

$$
\begin{aligned}
& D_{\mathrm{KL}}\Big(\mathrm{Dir}(\alpha_1^q,\overset{n+1}{\ldots},\alpha_{n+1}^q) \parallel \mathrm{Dir}(\alpha_0^{p'}\tfrac{\alpha_1^q}{\alpha_0^q},\overset{n+1}{\ldots},\alpha_0^{p'}\tfrac{\alpha_{n+1}^q}{\alpha_0^q})\Big) \\
& +\sum_{i=1}^{n+1} D_{\mathrm{KL}}\Big(\mathrm{Dir}(\tfrac{\alpha_i^q}{\kappa_i},\overset{\kappa_i}{\ldots},\tfrac{\alpha_i^q}{\kappa_i}) \parallel \mathrm{Dir}(\alpha_0^{p'}\tfrac{\alpha_i^q}{\alpha_0^q\kappa_i},\overset{\kappa_i}{\ldots},\alpha_0^{p'}\tfrac{\alpha_i^q}{\alpha_0^q\kappa_i})\Big) \\
& \quad = \log\frac{\Gamma(\alpha_0^q)}{\Gamma(\alpha_0^{p'})} - \sum_{i=1}^{n+1}\kappa_i \log\frac{\Gamma(\frac{\alpha_i^q}{\kappa_i})}{\Gamma(\frac{\alpha_0^{p'}\alpha_i^q}{\alpha_0^q\kappa_i})} + (1-\tfrac{\alpha_0^{p'}}{\alpha_0^q})\sum_{i=1}^{n+1}\alpha_i^q(\psi(\tfrac{\alpha_i^q}{\kappa_i})-\psi(\alpha_0^q))
\end{aligned}
$$

Now we can put all these pieces together.

$$
\begin{aligned}
& D_{\mathrm{KL}}(\mathrm{BFDP}(\boldsymbol{G}^q,\boldsymbol{\alpha}^q,\boldsymbol{\kappa}) \parallel \mathrm{BFDP}(\boldsymbol{G}^p,\boldsymbol{\alpha}^q\tfrac{\alpha_0^{p'}}{\alpha_0^q},\boldsymbol{\kappa})) \\
& = \int_{\boldsymbol{\rho}}\int_{\boldsymbol{\pi}'}\int_{\boldsymbol{v}} d(\boldsymbol{\rho};\alpha_1^q,\ldots,\alpha_{n+1}^q)\left(\prod_{i=1}^{n+1} d(\boldsymbol{\pi}_i';\tfrac{\alpha_i^q}{\kappa_i},\overset{\kappa_i}{\ldots},\tfrac{\alpha_i^q}{\kappa_i})\prod_{i=1}^{n+1}\prod_{j=1}^{\kappa_i} G_i^q(\boldsymbol{z}_{ij})\right)\log\frac{\mathrm{BFDP}(\boldsymbol{G}^p,\boldsymbol{\alpha}^q\frac{\alpha_0^{p'}}{\alpha_0^q},\boldsymbol{\kappa})}{\mathrm{BFDP}(\boldsymbol{G}^q,\boldsymbol{\alpha}^q,\boldsymbol{\kappa})}\, d\,\boldsymbol{\rho}\, d\,\boldsymbol{\pi}'\, d\,\boldsymbol{v} \\
& = D_{\mathrm{KL}}\Big(\mathrm{Dir}(\alpha_1^q,\overset{n+1}{\ldots},\alpha_{n+1}^q) \parallel \mathrm{Dir}(\alpha_0^{p'}\tfrac{\alpha_1^q}{\alpha_0^q},\overset{n+1}{\ldots},\alpha_0^{p'}\tfrac{\alpha_{n+1}^q}{\alpha_0^q})\Big) \\
& \quad +\sum_{i=1}^{n+1} D_{\mathrm{KL}}\Big(\mathrm{Dir}(\tfrac{\alpha_i^q}{\kappa_i},\overset{\kappa_i}{\ldots},\tfrac{\alpha_i^q}{\kappa_i}) \parallel \mathrm{Dir}(\alpha_0^{p'}\tfrac{\alpha_i^q}{\alpha_0^q\kappa_i},\overset{\kappa_i}{\ldots},\alpha_0^{p'}\tfrac{\alpha_i^q}{\alpha_0^q\kappa_i})\Big) + \kappa_i D_{\mathrm{KL}}(G_i^q \parallel G_0^p) \\
& = \log\Gamma(\alpha_0^q)-\log\Gamma(\alpha_0^{p'})+\sum_{i=1}^{n+1}\kappa_i(\log\Gamma(\frac{\alpha_0^{p'}\alpha_i^q}{\alpha_0^q\kappa_i})-\log\Gamma(\tfrac{\alpha_i^q}{\kappa_i}))+(\alpha_0^q-\alpha_0^{p'})\left(-\psi(\alpha_0^q)+\sum_{i=1}^{n+1}\tfrac{\alpha_i^q}{\alpha_0^q}\psi(\tfrac{\alpha_i^q}{\kappa_i})\right) \qquad (13) \\
& \quad +\tfrac{1}{2}\sum_{i=1}^{n+1}\kappa_i\sum_{h=1}^{d}(\frac{(\mu_{ih}^q-\mu_h^p)^2}{(\sigma_h^p)^2}+\frac{(\sigma_{ih}^q)^2}{(\sigma_h^p)^2}-\log\frac{(\sigma_{ih}^q)^2}{(\sigma_h^p)^2}-1)
\end{aligned}
$$

Equation equation 13 gives the KL portion of the loss when we are given the full set $\boldsymbol{\kappa}$ of numbers of vectors κ_i generated for each component i.

Equation equation 13 is approximately linear in κ_i, when the variation in κ_i is fairly small relative to the values of κ_i. The Gaussian term is exactly linear in κ_i, and the terms $\psi(\frac{\alpha_i^q}{\kappa_i})$ and $\kappa_i\Big(\log\Gamma(\frac{\alpha_i^q}{\alpha_0^q\kappa_i})-\log\Gamma(\frac{\alpha_i^q}{\kappa_i})\Big)$ are both approximately linear in κ_i. This allows us to approximate the expectation over κ_i of this loss as this loss of the expectation over κ_i, as discussed in Section 3.1. In this case, this approximation of the full KL divergence is:

$$
\begin{aligned}
& D_{\mathrm{KL}}(\mathrm{BFDP}(\boldsymbol{G}^q,\boldsymbol{\alpha}^q,\boldsymbol{\kappa}) \parallel \mathrm{BFDP}(\boldsymbol{G}^p,\boldsymbol{\alpha}^q\tfrac{\alpha_0^{p'}}{\alpha_0^q},\boldsymbol{\kappa})) \\
& \approx \log\Gamma(\alpha_0^q)-\log\Gamma(\alpha_0^{p'})+(\alpha_0^q-\alpha_0^{p'}))\Big(\psi(\tfrac{\alpha_0^q}{\kappa_0})-\psi(\alpha_0^q)\Big)+\kappa_0\left(\log\Gamma(\frac{\alpha_0^{p'}}{\kappa_0})-\log\Gamma(\frac{\alpha_0^q}{\kappa_0})\right) \qquad (14) \\
& \quad +\tfrac{1}{2}\kappa_0\sum_{i=1}^{n+1}\frac{\alpha_i^q}{\alpha_0^q}\sum_{h=1}^{d}\left(\frac{(\mu_{ih}^q-\mu_h^p)^2}{(\sigma_h^p)^2}+\frac{(\sigma_{ih}^q)^2}{(\sigma_h^p)^2}-1-\log\frac{(\sigma_{ih}^q)^2}{(\sigma_h^p)^2}\right)
\end{aligned}
$$

J REPARAMETERISATION TRICK AND SAMPLING

In this section we consider the reparameterisation trick to allow back propagation through the sampling step. We consider the Gaussian base distribution and DP weights seperately.

J.1 SAMPLING VECTORS FROM A COMPONENT OF THE BASE DISTRIBUTION

Each vector $\boldsymbol{z}_k$ is sampled independently from some specific component G_i^q of the base distribution G_0^q. Since we assume that all these components are distributed according to a Gaussian $G_i^q = \mathcal{N}(\boldsymbol{\mu}_i^q, \boldsymbol{I}(\boldsymbol{\sigma}_i^q)^2)$, we can sample from this distribution using location-scale shifting (Kingma & Welling, 2014):

$$\begin{aligned} \boldsymbol{z}_k &= \boldsymbol{\mu}_i^q + \boldsymbol{\sigma}_i^q \epsilon_k \\ \epsilon_k &\sim \mathcal{N}(\mathbf{0},\mathbf{1}) \end{aligned} \tag{15}$$

Since the random sampling comes from an unparameterised unit Gaussian, there is no need to backpropagate error into this sampling step, but the error can be backpropagated into $\boldsymbol{\mu}_i^q$ and $\boldsymbol{\sigma}_i^q$ given a specific sample. This is the reparameterisation trick for Gaussian distributions.

J.2 SAMPLING FROM A DIRICHLET DISTRIBUTION

A Dirichlet distribution over category weights can be sampled by sampling from a Gamma distribution for each category and then normalising. A sum-normalised set of κ random variables $\pi_1,...,\pi_\kappa \sim Dir(\alpha_1,...,\alpha_\kappa)$ follows a Dirichlet distribution if the unnormalised random variables γ_i each follow a Gamma distribution.

$$\begin{aligned} \pi_i &= \frac{\gamma_i}{\sum_i^\kappa \gamma_i} \\ \gamma_i &\sim \Gamma(\alpha_i, \beta{=}1) \end{aligned} \tag{16}$$

where $\Gamma(\alpha_i,\beta{=}1)$ is the Gamma distribution with $\beta{=}1$, whose PDF is $f(x) = \frac{1}{\Gamma(\alpha_i)} \exp((\alpha_i - 1)\log(x) - x)$. There is no closed-form explicit reparameterisation trick for the exact Gamma distribution, but there are for approximations. We propose to use a combination of two approximations for the Gamma distribution which have a reparameterisation trick, one for small values of α_i and one for larger values of α_i.[5]

Inverse CDF approximation to Gamma distributions The Gamma distribution cannot use location-scale shifting for sampling due to its asymmetry, nor can the parameters and noise components be decoupled in the inverse CDF. Hence, (Knowles, 2015) suggests sampling using an approximation to the inverse CDF of the Gamma distribution of the following form:

$$\begin{aligned} \gamma_i &\approx \beta^{-1}(u_i \alpha_i \Gamma(\alpha_i))^{1/\alpha_i}, \\ u_i &\sim \mathrm{U}(0,1). \end{aligned} \tag{17}$$

This approximation allows the inverse CDF of the Gamma distribution to be a function of the parameters and independent noise from a uniform distribution $\mathrm{U}(0,1)$. However, this approximation is only recommended when the value of $\alpha_i < 1$ and $\beta = 1$. In our case $\beta = 1$ but we sometimes have large α_i.

Gaussian approximation to Gamma distributions Knowles (2015) further mentions that the Gaussian distribution can be used to approximate a Gamma distribution for larger α. Bahuleyan et al. (2017) uses a similar approach to approximate variational attention weights. The Gaussian distribution is a symmetric distribution which can be sampled by location-scale shifting, as discussed above. The Gamma distribution $\Gamma(\alpha,\beta{=}1)$ can be approximated with a Gaussian of the form $\gamma \sim \mathcal{N}(\alpha, \sqrt{\alpha})$ (Knowles, 2015), which gives us:

$$\begin{aligned} \gamma_i &\approx \alpha_i + \sqrt{\alpha_i}\epsilon_i \\ \epsilon_i &\sim \mathcal{N}(0,1) \end{aligned} \tag{18}$$

[5] We leave the investigation of implicit reparameterisation gradients (Figurnov et al., 2018) to future work. This approach is an alternative to explicit reparameterisation for cases like Gamma distributions, but first we investigate the approach which is more standard in the VAE literature.

The Gaussian distribution is symmetric and can take on negative values. Hence, this approximation is inappropriate for the Gamma distribution unless the α_i parameter is sufficiently large, otherwise the sample will need to be truncated to a value greater than zero.

The combined reparameterisation of Gamma distributions To visualise the error for these two approximations, their average L_1 distance from the true Gamma inverse CDF is plotted in Figure 9 for different values of α. The plot shows that the approximation error is equal when $\alpha = 0.6363$. To take advantage of the strengths of both these approximations, we propose to reparameterise the Gamma distribution as a blend of these two approximations with a switch at $\alpha = 0.6363$ and truncate negative samples to zero.

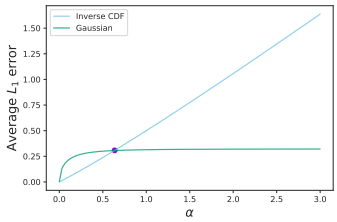

Figure 9: The average absolute difference between a Gamma inverse CDF function and our approximations: inverse CDF approximation and Gaussian inverse CDF are plotted for values of α.

K Practical Implementation

In this section we provide the equations used to allow denoising attention to be implemented in a deep learning framework at training time and test time.

Denoising Attention at Training Time During training the set of vectors $\boldsymbol{Z} \in \mathbb{R}^{n \times p}$ are sampled and outputted by the NVIB layer. The query $\boldsymbol{u'} \in \mathbb{R}^{1 \times p}$ is projected by the grouped matrices $\boldsymbol{W}^Q, \boldsymbol{W}^K \in \mathbb{R}^{p \times d}$ to such that $\boldsymbol{u} = (\boldsymbol{u'}\boldsymbol{W}^Q(\boldsymbol{W}^K)^T)$. The probability values $\log(\boldsymbol{\pi}) \in \mathbb{R}^{1 \times p}$ are sampled from the NVIB layer. The keys' dimensionality d is for scaling.

$$DAttn(\boldsymbol{u}; F_{\boldsymbol{Z}}) \quad = \quad \text{softmax}\Big(\tfrac{1}{\sqrt{d}}\boldsymbol{u}\boldsymbol{Z}^T + \log(\boldsymbol{\pi}) - \tfrac{1}{2\sqrt{d}}\|\boldsymbol{Z}\|^2\Big)\boldsymbol{Z},$$

We define this for $\boldsymbol{u} \in \mathbb{R}^{1 \times p}$ however, this can easily extend to multiple queries.

Denoising Attention at Test Time During test time we do not sample $\boldsymbol{Z} \in \mathbb{R}^{n \times p}$ but rather use the mean posterior distribution. We use the posterior mean $\boldsymbol{\mu}^q \in \mathbb{R}^{n \times p}$ and posterior variance parameters $(\boldsymbol{\sigma}^q)^2 \in \mathbb{R}^{n \times p}$

$$\begin{aligned} &DAttn(\boldsymbol{u}, \boldsymbol{\mu}^q, \boldsymbol{\sigma}^q\,; \boldsymbol{\mu}^p, \boldsymbol{\sigma}^p) \\ &= \quad \text{softmax}\left(\boldsymbol{u}(\frac{\boldsymbol{\mu}^q}{(\boldsymbol{\sigma}^p)^2})^T + \log(\frac{\boldsymbol{\alpha}^q}{\boldsymbol{\alpha}_0^q}) - \left(\frac{1}{2}\left\|\frac{\boldsymbol{\mu}^q}{\boldsymbol{\sigma}^p}\right\|^2\right)^T - \mathbf{1}_p(\log(\boldsymbol{\sigma}^p))^T\right)\left(\frac{(\boldsymbol{\sigma}^q)^2}{(\boldsymbol{\sigma}^p)^2} \odot (\mathbf{1}_n^T\boldsymbol{u}) + \frac{\sqrt{d}}{(\boldsymbol{\sigma}^p)^2} \odot \boldsymbol{\mu}^q\right), \end{aligned}$$

A caveat of this derivation is that applies simply for single-head attention and is not trivial to apply for multi-head attention. We leave this for future work.